Microporous Titanosilicates and other Novel Mixed Octahedral-Tetrahedral Framework Oxides

João Rocha*[a] and Michael W. Anderson[b]

Keywords: Zeolites / Microporous zeolites / Titanosilicates / Transition metal

Stable microporous materials, such as zeolites, are extremely important for applications in catalysis, adsorption, ion-exchange, and separation. In this review we describe a new class of stable microporous materials that involves novel mixed octhaedral-tetrahedral framework oxides. The archetypal material is based on titanosilicates, although there is tremendous scope for introducing many other transition metals. These materials not only have potential novel applications in the fields normally associated with zeolites but also possible applications in the areas of optoelectronics, nonlinear optics, batteries, magnetic materials and sensors.

Introduction

Zeolites are crystalline, hydrated aluminosilicates with open three-dimensional structures built of $[SiO_4]^{4-}$ and $[AlO_4]^{5-}$ tetrahedra linked to each other by sharing all the oxygens to form regular intracrystalline cavities and channels of molecular dimensions.[1–3] Silicon-oxygen tetrahedra are electrically neutral when connected together in a three-dimensional network as in quartz (SiO_2). The replacement of Si^{IV} by Al^{III} in such a structure creates an electrical imbalance and, to preserve overall electrical neutrality, each AlO_4 tetrahedron needs a balancing positive charge. This is provided by exchangeable cations held electrostatically within the zeolite. Zeolites possess remarkable physical and

[a] Department of Chemistry, University of Aveiro
3810 Aveiro, Portugal
Fax: (internat.) + 351-234/370-084
E-mail: rocha@dq.ua.pt
[b] UMIST Centre for Microporous Materials, Department of Chemistry,
P. O. Box 88, Manchester M60 1QD, UK
Fax: (internat.) + 44-161/236-7677
E-mail: m.anderson@umist.ac.uk

João Rocha was born in Portugal in 1962. Following his undergraduate studies in Physics and Chemistry at Aveiro University he became assistant in the Department of Chemistry of this University in 1985. In 1987 he joined the group of Jacek Klinowski in Cambridge. His Ph.D. thesis was entitled solid-state NMR studies of kaolinite and related materials and concentrated on the study of the important clay mineral kaolinite and related high-temperature phases.
This was followed by a post-doctoral appointment in Cambridge, still in the group of J. Klinowski, working on solid-state NMR of zeolitic materials. He was appointed Lecturer in Chemistry at University of Aveiro in 1991 and promoted to Professor of Inorganic Chemistry in 1999 and currently heads the Inorganic and Materials Chemistry Centre and the solid-state NMR laboratory. His research interests include: synthesis and characterisation of novel microporous materials; development of new materials for optoelectronics; NMR characterisation of wood and lignocellulosic materials; development of new solid-state NMR techniques for the study of quadrupolar nuclei.

Michael W. Anderson was born in Wimbledon, U.K., in 1960. Following his undergraduate studies in Chemical Physics at Edinburgh University he joined the group of John M. Thomas in Cambridge in 1981. His Ph.D. thesis was entitled Dealuminated Zeolites and concentrated on the removal of aluminium from zeolites using $SiCl_4$. This was followed by three post-doctoral appointments: University of Houston with Larry Kevan working on pulsed EPR measurements of transition metals in zeolites; University of Connecticut with Steve Suib working on catalyst poisoning; University of Cambridge with Jacek Klinowski where he developed in situ NMR methods for monitoring catalytic events in zeolites. He was appointed Lecturer in Chemistry at UMIST in 1990 and promoted to Professor of Materials Chemistry in 1998 and is currently Director of the UMIST Centre for Microporous Materials. His research interests include: experimental and theoretical NMR studies of heterogeneous catalysts; structural studies of mesoporous materials; atomic force microscopy and electron microscopy studies of crystallisation mechanisms; synthesis and applications of novel microporous materials.

MICROREVIEWS: This feature introduces the readers to the authors' research through a concise overview of the selected topic. Reference to important work from others in the field is included.

  1434–1948/00/0505–0801 $ 17.50+.50/0

chemical properties. The most important chemical properties are selective sorption, ion exchange and catalytic activity.

During the 1980s a variety of novel microporous framework structures were synthesised based on an aluminophosphate system.[4] In their pure form the aluminophosphates are termed AlPOs and consist of alternating corner-sharing framework $[AlO_4]^{5-}$ and $[PO_4]^{3-}$ tetrahedral groups. Overall the frameworks have no net charge and, consequently, no cation-exchange properties and little catalytic potential. Framework substitutions are, however, possible and lead to silico-aluminophosphates[5] (SAPOs) and metal-substituted aluminophosphates (MeAPOs).[6] Some of these new materials have the framework topologies of known zeolites while others may have novel structures. In all these materials the framework metal atoms are ostensibly in tetrahedral coordination, although under certain circumstances (for example, various hydration conditions) the coordination might change to five- or six-fold. Porous structures comprised entirely of octahedral sites have also been generated. For example, the manganese oxides known as OMS materials contain only octahedral framework atoms.[7a]

A third, much less explored, compositional possibility for microporous frameworks are structures consisting of interlinked octahedra and tetrahedra. Although clays and related materials, in some way, fall into this category, they only possess two-dimensional co-valent connectivity. Three-dimensional connectivity is required to impart substantial structural stability and we are only concerned with such networks in this review. In 1990 Chapman and Roe were already well aware of the importance of these mixed framework materials.[8] In their words: ''While new structures and compositions of molecular sieves continue to be synthesised, there are indications that attention is turning toward a potentially large class of novel molecular sieve materials composed of interconnected octahedral- and tetrahedral-oxide polyhedra. Such materials will most likely provide examples of new topologies and novel compositions''. In this microreview it is our endeavour to show that some of the most interesting and important developments in the field of zeolites and zeotype materials are taking place in the area of mixed octahedral-tetrahedral oxides. Here, we shall only address the chemistry of silicates and will not be concerned with, in particular, the burgeoning and exciting chemistry of porous phosphates.[7b]

Synthesis

The synthesis of microporous titanosilicates[8–11] and other novel zeotype materials is usually carried out in Teflon-lined autoclaves under hydrothermal conditions with temperatures ranging from ca. 150 to 230 °C and times varying between a few hours and ca. 30 days. In certain cases, the materials have been prepared at relatively high temperatures. For example, single crystals of a titanosilicate analogue of the mineral pharmacosiderite, $Cs_3HTi_4O_4(SiO_4)_3 \cdot 4\,H_2O$, have been obtained hydrothermally in a sealed gold tube at 750 °C for 40 h.[12] The pH of the synthesis gel is normally high, in the range 10–13. Seeding the gel with a small amount of the desired phase (or even with a related solid) is a common practice. The syntheses are in general driven by kinetics, with different metastable phases being formed with time. So far, most research has concentrated on the synthesis of microporous titanosilicates. The experience gathered in this field is guiding the efforts aimed at other systems, most notably zirconosilicates. Hence, here we shall discuss in more detail the synthesis of microporous titanosilicates, particularly ETS-10 (*E*ngelhard *t*itano*s*ilicate material number 10).

The synthesis of ETS-10 was first reported by Kuznicki in 1989.[9] The titanium source used was $TiCl_3$. A slight modification of this method afforded highly crystalline and pure ETS-10 suitable for structural elucidation.[13,14] $TiCl_4$ is another much used (and cheaper) titanium source. For example, using this precursor Das et al.[15] reported a method for the rapid (< 16 h) synthesis of ETS-10. Liu and Thomas[16] have shown that under proper conditions the thermodynamically stable TiO_2 phases of anatase and rutile can be used as suitable titanium sources for the synthesis of porous titanosilicates. A few organotitanium compounds have also been used to prepare microporous titanosilicates. Because they are very sensitive to moisture, these compounds are difficult to handle and require special facilities for their transfer during the gel preparation. For example, Chapman and Roe[8] used $Ti(OC_2H_5)_4$ in the preparation of GTS-1 while Clearfield and co-workers synthesised a novel porous titanosilicate using titanium isopropoxide.[17] Sodium silicate solutions and fumed and colloidal silica are suitable silicon sources. Organosilicon compounds, such as tetraethylorthosilicate have also been used.[17] The synthesis of ETS-10 usually (although not always) requires the presence in the parent gel of both Na^+ and K^+ ions. Other phases, such as some of the AM (*A*veiro/*M*anchester) materials[18] are produced in a pure state only when a single type of cation is present. Potassium fluoride is often used for preparing ETS-10 but its presence is not crucial. A comprehensive study of the hydrothermal synthesis conditions which yield pure and highly crystalline ETS-10 from $TiCl_3$ and anatase has been reported.[19] This work examines the influence on the synthesis of the following parameters: presence of fluoride, sodium, and potassium ions, seeds, H_2O/Si and Si/Ti molar ratios, parent gel pH, temperature, and time. A similar study has been carried out by Das et al., using $TiCl_3$ as the titanium source.[20]

Most porous titanosilicates and other related new materials reported to date can be synthesised without the addition of any organic template molecules. However, several groups have prepared ETS-10 with a range of templates: tetramethylammonium chloride,[21,22] pyrrolidine, tetraethylammonium chloride, tetrapropylammonium bromide,1,2-diaminoethane,[22] choline chloride, and the bromide salt of hexaethyl diquat-5.[23] From the point of view of industrial synthesis scale-up it is very important that many of the new structures can be synthesised in the absence of

costly templating agents. Furthermore, the occluded templates usually need to be removed following synthesis in order to impart microporosity, a procedure that can be both costly and potentially damaging to the framework.

The framework substitution of titanium and silicon by other elements requires a judicious choice of the respective source, which is usually introduced in the parent synthesis gel. The following sources of aluminium, gallium, niobium, and boron for element insertion in the ETS-10 framework have been reported: $NaAlO_2$,[24] $GaCl_3$,[25] $Nb(HC_2O_4)_5$,[26] and $Na_2B_2O_4$[27] (see also refs.[28,29]). In the synthesis of microporous zirconosilicates $ZrCl_4$[30–32] and $Zr(OC_3H_7)_4$[33] have been used as the zirconium sources. The vanadosilicate AM-6, a structural analogue of ETS-10, has been prepared from $VOSO_45H_2O$.[34]

Structure

ETS-10

In 1990 Chapman and Roe published the synthesis and X-ray diffraction pattern of a microporous titanosilicate[8,11] that seemed to have the structure of the mineral zorite by comparison of the diffraction patterns. At about the same time Engelhard Corporation filed a series of patents describing a similar small-pore material, which they named ETS-4 (*E*ngelhard *t*itano*s*ilicate-4) and another wide-pore titanosilicate material named ETS-10.[9,10] Owing to its wide-pore nature and thermal stability ETS-10 is arguably the most important octahedral/tetrahedral framework microporous titanosilicate to be synthesised to date. Consequently, it is important to understand the structure of this material in some detail.

The structure of ETS-10 was solved and reported briefly in 1994 by Anderson et al.[13] and described fully by the same group the following year.[14] Two problems prevented an easy solution to the structure of ETS-10: first, the material could only be synthesised as a powder and, more importantly, the material was inherently disordered. Consequently, conventional diffraction techniques to solve the structure proved inadequate. The following strategy was therefore adopted to elucidate the structure of ETS-10: (i) target the framework ring connectivity and local disorder with high-resolution electron microscopy (HREM); (ii) determine the atomic make-up of the material by chemical analysis; (iii) determine the local silicon environment using ^{29}Si solid-state nuclear magnetic resonance (NMR); (iv) refine a trial structure using a distance-least-squares (DLS) analysis of bond angles and bond lengths; (v) combine the refined structure and known disorder to simulate powder X-ray diffraction data.

The typical crystal morphology of ETS-10 is shown in Figure 1. These scanning electron micrograph images show that (i) the particle has a pseudo-4-fold symmetry along an axis indicated by the large arrow; (ii) traces of faults that are perpendicular to the axis and are indicated by small arrows. This faulted structure is always present in ETS-10 and Figure 1 represents a high quality material.

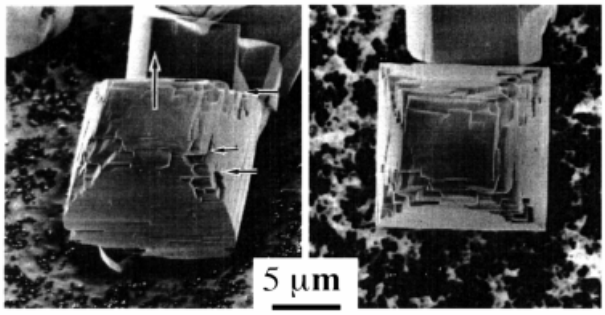

Figure 1. Scanning electron micrograph of a high-quality ETS-10 sample; large arrow depicts pseudo 4-fold axis, small arrows indicate faulting caused be intergrowths

The details of the inherent disorder and the pore structure in ETS-10 are most clearly revealed in the high-resolution electron micrograph (Figure 2). The large 12-ring pores are clearly visible. In order to discern the disorder the reader should note the stacking of these large pores from the bottom of the micrograph to the top. It will be seen that the pores stack randomly to the right or to the left.

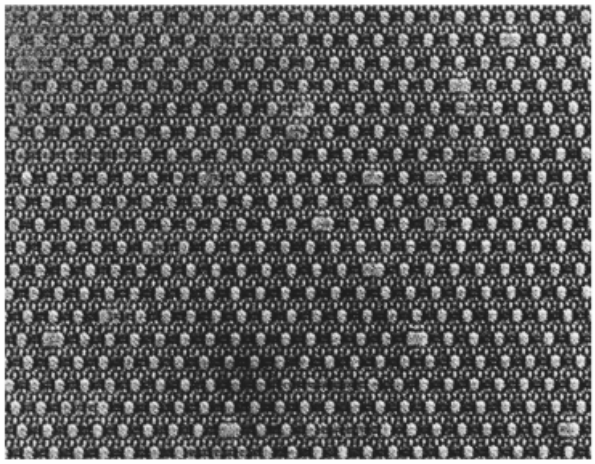

Figure 2. High-resolution electron micrograph of ETS-10

The most interesting aspect of the structure of ETS-10 is that it contains infinite –O–Ti–O–Ti–O– chains (with alternating long/short bonds[35]) that are surrounded by a silicate ring structure. These combine to make up a rod (Figure 33a and 3b) and it is this rod nature that imparts some of the interesting optical properties described in the applications section. Adjacent layers of rods are stacked orthogonal to each other (Figure 3c). These double layers are then stacked with a displacement of 1/4 unit cell in either the [100] direction or the [010] direction to give four possible connections (Figure 3d). If these four possible connections are given equal probability and the stacking is random then the disordered ETS-10 structure is constructed. The pore structure of ETS-10 has 12-rings in all three dimensions; these are straight along [100] and [010] and crooked along the direction of disorder. However, there are only a handful of microporous zeolitic materials with a 3-dimensional 12-ring pore system and in this respect ETS-10 has

excellent diffusion characteristics. It should be noted that the crooked channel is not blocked or the pore volume reduced by the disorder.

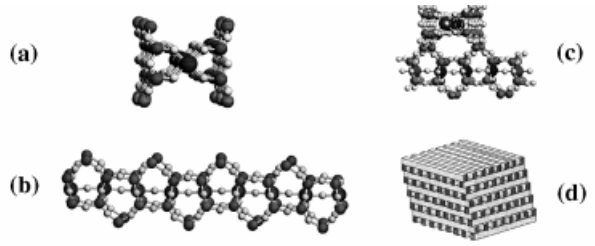

Figure 3. Structural make-up of ETS-10: (a) and (b) show the same rod section of ETS-10 in orthogonal views – large spheres Ti, medium spheres Si and small spheres O; (c) shows how these rods link; (d) shows one possible ordered arrangement of these orthogonol rods

It is interesting to conjecture whether it is possible to construct ordered variants of the ETS-10 structure. The lattice energy difference between different stacking sequences is minimal, however, different sequences result in different pore architecture. A zig-zag stacking of pores results in chiral symmetry and a spiral 12-ring pore in the third dimension. In order to synthesise such a material no doubt a chiral organic templating agent would be required but as yet this has not been achieved.

Mistakes in the stacking sequences (which occur frequently, probably as a result of the crystal growth mechanism) result in line defects in ETS-10 which are in effect double-sized pores. A schematic of the framework connectivity and the incorporation of defects is shown in Figure 4.

The framework formula of this basic unit is $Si_{40}Ti_8O_{104}^{16-}$, which is counterbalanced by 16 monovalent cations. In this original structural work it was impossible to locate the cations in ETS-10. The as-prepared material is 1/4 K^+ and 3/4 Na^+. The most likely location of the cations has been determined by a combination of molecular modelling and, for sodium, ^{23}Na solid-state NMR. Figure 5 shows the final structure of ETS-10 with the cations principally located in sites adjacent to the titanate chains where they balance the charge on the titanium centres.

Very recently a single crystal study on ETS-10 has refined a superposition cell, which essentially regards the structure as a combination of all the ordered variants and confirms in essence all of the previous structural work.[36]

ETS-4

Similar to ETS-10 the nominal structure of ETS-4 suggests that it could have very interesting applications. As noted above, the powder X-ray diffraction pattern of ETS-4 suggests strong similarities with the structure of the natural mineral zorite. In 1973 a naturally occurring alkaline titanosilicate identified as zorite was discovered[37] in trace quantities on the Siberian Tundra. The structure solution of this mineral was published[38] six years later in an article

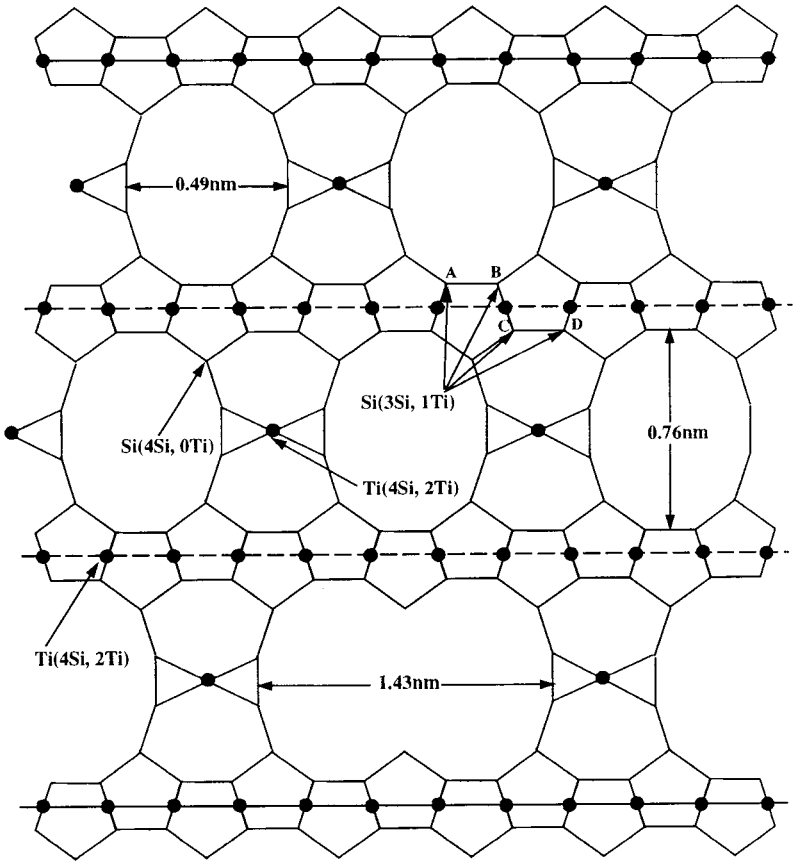

Figure 4. Framework connectivity in ETS-10 showing different chemical and crystallographic environments; also shown is the incorporation of large defects as double pores

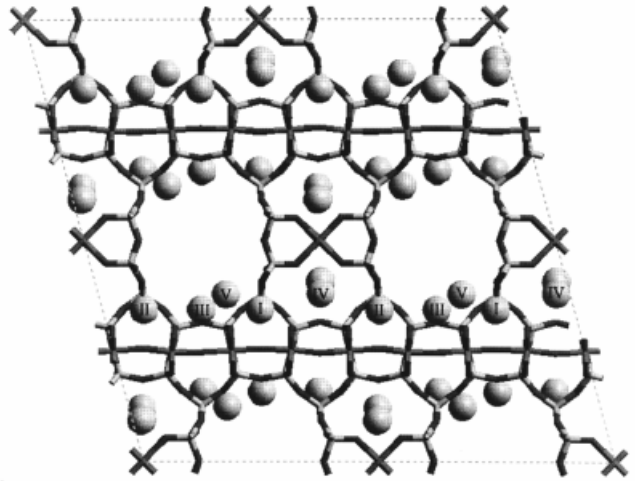

Figure 5. Five cation sites in ETS-10 and their relationship to the framework

entitled "The OD structure of Zorite". According to this contribution,[38] the structure of this mineral is characterised by a highly disordered framework with ostensibly a 2-dimensional channel system. Two orthogonal sets of channels are defined by 12-T/O atom and 8-T atom rings (T = *t*etrahedral silicon; O = *o*ctahedral titanium). In reality, the disorder in zorite results in the larger 12-ring channels becoming partitioned into sections. A molecule diffusing into this 12-T/O ring channel must make detours through the 8-T ring channel system in order to pass freely. Consequently, the adsorption characteristics of zorite are far inferior to that expected for an unfaulted material. Furthermore, zorite lacks thermal stability as internal water acts as part of the structure forming chains through the channel system. When the water is removed the framework structure collapses. Figure 6 shows the framework structure of zorite with possible stacking sequences of ordered end member polymorphs.

In zorite the titanium exists in two different chemical environments, titania rods similar to those in ETS-10, and isolated titania semi-octahedra, which are exposed to the channel system. Consequently, if ETS-4 has the structure of zorite then the accessibility of the titanium centres to the channel system may be a benefit for certain applications, despite the stability issue. The only outstanding problem with the structure of ETS-4 is that the ^{29}Si MAS-NMR spectrum does not agree with the crystal structure. The crystal structure dictates two Si environments Si(2Si,2Ti) and Si(3Si,1Ti) in a ratio of 2:1. The ^{29}Si MAS-NMR spectrum displays two signals, although these are not in the correct ratio. It is still unclear at present how this discrepancy arises but the most reasonable suggestion is that it is due to a large number of defect sites in ETS-4.[39,40]

In terms of stability, the structure of zorite or ETS-4 contains structural water bound in chains along the channel system. At temperatures of 200 °C this water is lost and the structure collapses. At temperatures above 700 °C there is a phase transformation into the dense titanosilicate structure narsarsukite.[41] Because the stoichiometry of ETS-4 and

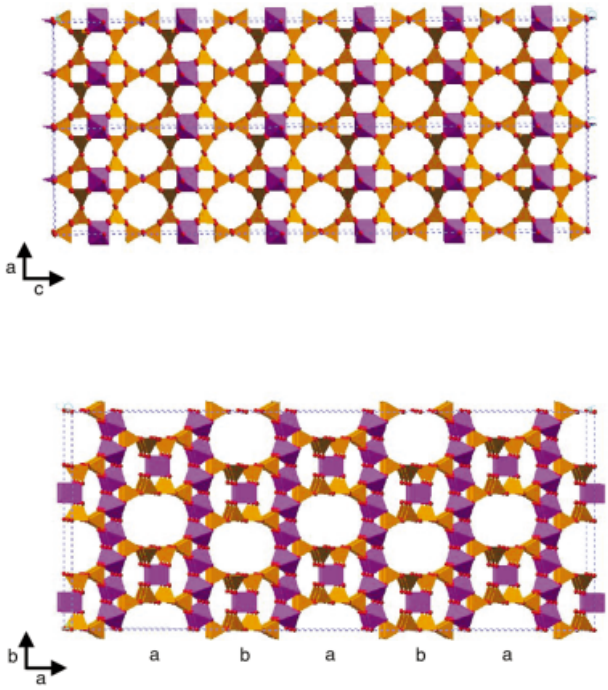

Figure 6. Two orthogonal projections of one possible ordered variant of ETS-4; purple Ti octahedra, brown Si tetrahedra, red spheres oxygens

narsarsukite are different, a quantity of silica must be added to ETS-4 in order to prepare pure narsarsukite at high temperatures.

Other Titanosilicates

In 1994 Clearfield and co-workers reported the synthesis, crystal structure, and ion-exchange properties of a novel porous titanosilicate of ideal composition $Na_2Ti_2O_3SiO_4 \cdot 2\ H_2O$.[17] The structure of this material has been solved from powder X-ray data by ab initio methods. The titanium atoms occur in clusters of four, grouped about the 4_2 axis, and are octahedrally coordinated by oxygen atoms (Figure 7a and 7b). The silicate groups link the titanium clusters into groups of four arranged in a square of about 7.8 Å in length. These squares are linked to similar squares in the *c* direction by sharing corners to form a framework that encloses a tunnel. Half the Na^+ ions are located in the framework, coordinated by silicate oxygen atoms and water molecules. The remaining Na^+ ions reside in the cavity, although some of them are replaced by protons. The Na^+ ions within the tunnels are exchangeable, particularly by Cs^+ ions.

Chapman and Roe[8] have prepared a number of titanosilicate analogues of the mineral pharmacosiderite, a non-aluminosilicate molecular sieve with a framework composition $KFe_4(OH)_4(AsO_4)_3$. Later, Clearfield and co-workers studied by powder X-ray diffraction methods the structure of pharmacosiderite analogues with composition $HM_3Ti_4O_4(SiO_4)_3 \cdot 4\ H_2O$ (M = H^+, K^+, Cs^+).[42] Harrison et al. have been able to grow single crystals of the same cesium phase and solve its structure by single-crystal

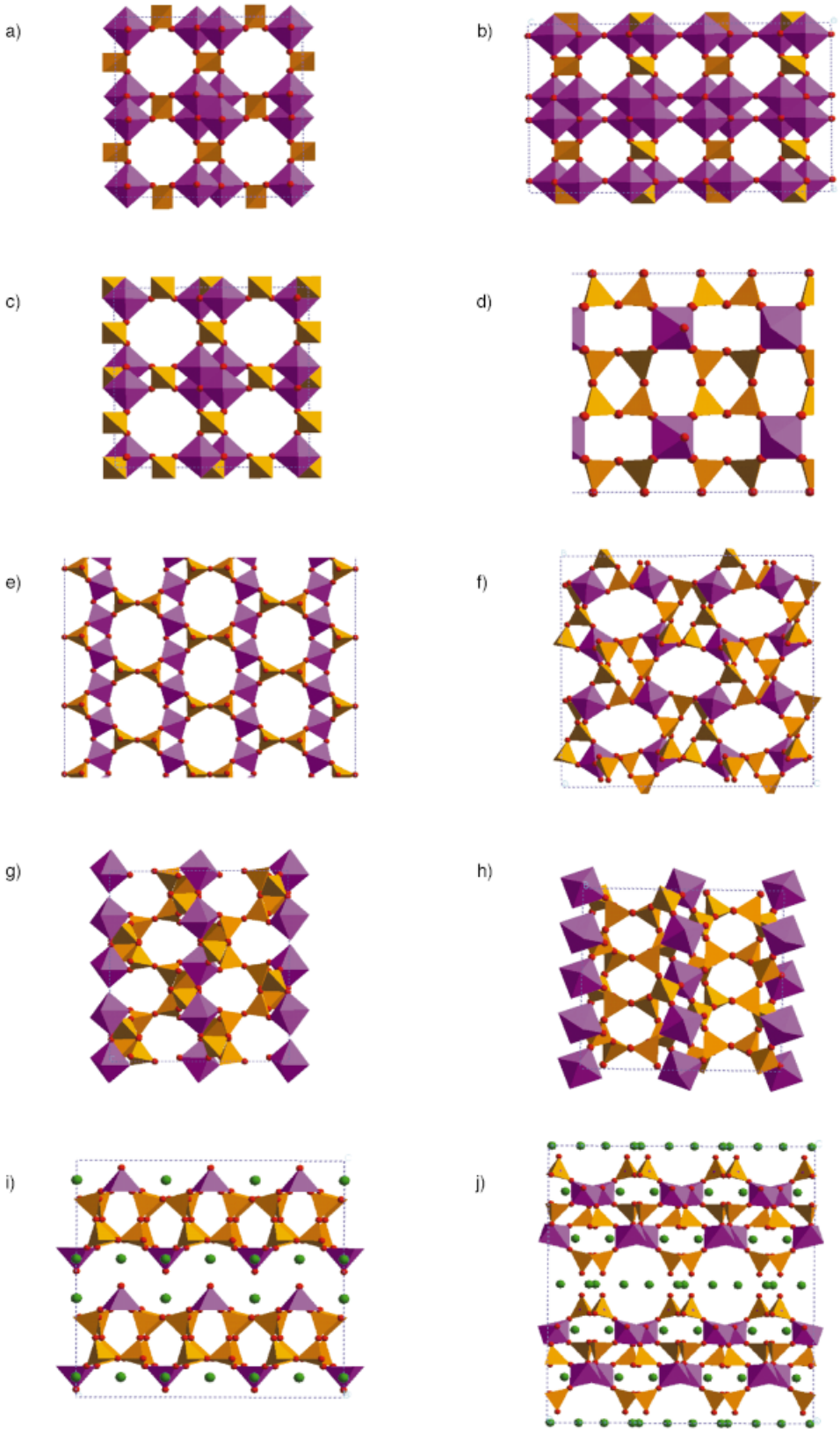

Figure 7. Projection of the structures of: (a) titanosilicate reported by Clearfield et al.[17] along the [001] and (b) [100] directions; (c) pharmacosiderite along [001]; (d) nenadkevichite along [100] and (e) [001]; (f) UND-1 along [100]; (g) penkvilksite 2*O* and AM-3 along [001] and (h) [010]; (i) AM-1 or JDF-L1 along [010]; (j) AM-4 along [100]; purple Ti octahedra, brown Si tetrahedra, green Na cations, red spheres oxygens

methods.[12] These materials possess a most interesting structure built up from TiO_6 octahedra, which share faces to form Ti_4O_4 cubes around the unit-cell corners and have silicate tetrahedra joining the titanium octahedra to form a three-dimensional framework (Figure 7c). Extra-framework Cs^+ species occupy sites slightly displaced from the centres of the intercage eight-ring windows, and also make $CsOH_2$ bonds to the water molecules that reside in the spherical cages.

Nenadkevichite is a rare mineral first found in the Lovozero region (Russia) with the composition $(Na,Ca)(Nb,Ti)Si_2O_7 \cdot H_2O$. The structure of nenadkevichite (from Saint-Hilaire, Quebec, Canada) consists of square rings of silicon tetrahedra Si_4O_{12} in the (100) plane joined together by chains of $(Nb,Ti)O_6$ octahedra in the [100] direction (Figure 7d and 7e).[43] The pores accommodate Na^+ in two partially (0.53 and 0.54) occupied sites and water molecules in two fully occupied sites. Rocha and Anderson and co-workers have been able to prepare a series of synthetic analogues of nenadkevichite with Ti/Nb molar ratios ranging from 0.8 to 17.1 and a purely titaneous sample.[44,45]

Many porous framework titanosilicates contain Ti–O–Ti linkages that often form infinite chains. Interestingly, the materials known as AM-2,[31,32,46–48] UND-1[49] and AM-3[46] do not contain any such linkages. AM-2 is a synthetic potassium titanosilicate analogue of the mineral umbite, a rare zirconosilicate found in the Khibiny alkaline massif (Russia).[50] Although the ideal formula of umbite is $K_2ZrSi_3O_9 \cdot H_2O$, a pronounced substitution of titanium for zirconium occurs. However, the natural occurrence of purely titaneous umbite is unknown. The successful synthesis of umbite materials with different levels of substitution of zirconium by titanium has been reported[31] and indicates the existence of a continuous solid solution that has not been described for any other sodium or potassium zirconosilicate. In the structure of umbite (not shown) the M octahedra, $(Zr,Ti)O_6$, and the T tetrahedra, SiO_4, form a three-dimensional MT-condensed framework.[50] The M octahedron is coordinated to six T tetrahedra. In addition to the M–O–T bonds these tetrahedra also form T–O–T links with each other. The resulting T radical has an identity period of three T tetrahedra and forms an infinite chain. The structures of umbite and the material known as UND-1 ($Na_{2.7}K_{5.3}Ti_4Si_{12}O_{36} \cdot 4\,H_2O$) are very similar.[49] The structure of UND-1 consists (Figure 7f) of six-membered rings of SiO_4 tetrahedra and isolated TiO_6 octahedra. Each TiO_6 octahedron connects, through corner-sharing, to six SiO_4 tetrahedra on the three six-membered rings, thus forming three three-membered rings, while each SiO_4 tetrahedron connects to two isolated TiO_6 octahedra and two other SiO_4 tetrahedra of the same six-membered ring. By such connections, channels running parallel to [100] are formed with eight-membered rings containing alternative –O–Si–O–Ti–O– linkages. The channel wall is covered by seven-membered rings (four SiO_4 tetrahedra and three TiO_6 octahedra) and three-membered rings. There are two cation sites in the structure. One is occupied only by K^+ and is located near the centre of the seven-membered ring of the wall. The other cation site is occupied by 33% K^+ and 67% Na^+ and is located in the large channel near the wall. AM-3 is a sodium titanosilicate analogue of the mineral penkvilksite found in Mont Saint-Hilaire, Québec (Canada), and the Kola Peninsula (Russia) with an ideal formula $Na_4Ti_2Si_8O_{22} \cdot 5\,H_2O$. The mineral occurs in two polytipic modifications, orthorhombic (penkvilksite-2*O*) and monoclinic (penkvilksite-1*M*).[51] These two polytypes have been described according to the OD theory as two of the four possible maximum degree of order polytypes within a family of OD structures formed by two layers.[51] Despite the different space group symmetries the 2*O* (*Pnca*) and 1*M* ($P2_1/c$) polytypes have the same atoms, labeled in the same way, in the asymmetric unit. They differ only in the stacking of the same building blocks. Thus, the following structure description (Figure 7 g and 7h) holds for both polytypes.[51] Penkvilksite contains two independent tetrahedra: The Si1-centred tetrahedra share two corners with other tetrahedra and two corners with TiO_6 octahedra; the Si2-centred tetrahedra share three corners with tetrahedra and one corner with a TiO_6 octahedron. Penkvilksite displays a new kind of connection among SiO_4 tetrahedra. Spirals of corner-sharing tetrahedra develop along [010] and have a periodicity of six tetrahedral units. The Si2-centred tetrahedra are shared between adjacent spirals, which are oriented in an alternate clockwise and counterclockwise fashion. The stacking of the layers along [001] gives rise to tetrahedral layers parallel to (100). The connection of neighbouring layers of tetrahedra is due to Ti^{IV} cations in an octahedral coordination. AM-3 is a synthetic analogue of penkvilksite-2*O*.[46] The synthesis of the 1*M* polytype has been reported recently by Liu et al.[52,53]

The synthesis of a few other microporous framework titanosilicates has also been reported. For example, Chapman and Roe have prepared a synthetic analogue of the mineral vinagradovite[8,54] with a framework composition $Na_8Ti_8Si_{16}O_{52}$. The structure of the mineral is composed of pyroxene chains joined to edge-sharing TiO_6 octahedra, which form brookite columns. These polyhedra define one-dimensional (4 Å) channels containing zeolitic water. A number of other minerals not yet prepared in the laboratory exhibit very interesting frameworks that are connected in a complex way (see the excellent review by J. V. Smith[55]). Verplanckite $[(Mn,Ti,Fe)_6(OH,O)_2(Si_4O_{12})_3]Ba_{12}Cl_9\{(OH,H_2O)_7\}$ has a framework with triple units of (Mn, Ti, Fe) in square-pyramidal coordination and four-rings of silicon tetrahedra.[56] The voids have a free diameter of 7 Å. Muirite, $Ba_{10}(Ca,Mn,Ti)_4Si_8O_{24}(Cl,OH,O)_{12} \cdot 4\,H_2O$, has edge-sharing trigonal prisms and eight-rings of SiO_4.[57]

When attempting to prepare novel microporous framework titanosilicates several groups have obtained layered materials, some of which have very interesting and unusual structures and show potential for being used in a number of applications such as ion exchange. One such material, known as AM-1[14,46] or JDF-L1,[58,59] has the composition $Na_4Ti_2Si_8O_{22} \cdot 4\,H_2O$. This is an unusual non-centrosymmetric tetragonal layered solid that contains five-coordin-

ated Ti^{IV} ions in the form of TiO_5 square pyramids in which each of the vertices of the base is linked to SiO_4 tetrahedra $[TiOO_4(SiO_3)_4]$ to form continuous sheets (Figure 7i).[59] The interlamellar Na^+ ions are exchangeable, for example by protonated alkylamines. AM-4, $Na_3(Na,H)Ti_2O_2[Si_2O_6]_2 \cdot 2\ H_2O$, is yet another example of a layered titanosilicate.[46,60] The crystal structure of AM-4 is built from TiO_6 (M) octahedra and SiO_4 (T) tetrahedra that form layers perpendicular to [001]. Each layer consists of a five-tier sandwich of T–M–T–M–T (Figure 7j). Between the layers are Na^+ cations and water molecules. The former also exist in small cages within the layers. The major features of the structure are zig-zag chains of edge-sharing TiO_6 octahedra running along the [100] direction that are connected together by corner-sharing pyroxene-type SiO_4 tetrahedra. Clearfield et al. reported the synthesis of a layered titanosilicate that seems to be closely related with AM-4.[61] The same group has also carried out a considerable amount of work on the evaluation of synthetic inorganic ion exchangers for cesium and strontium removal from contaminated groudwater and wastewater using (among other materials) several microporous and layered titanosilicates, some of which possess unknown structures (see, for instance, ref.[62] and references therein).

Zirconosilicates

Zirconium silicates occur widely in nature and their formation under hydrothermal conditions (from ca. 300 to 550 °C) has been given considerable attention, though mainly for the solution of general geophysical and mineralogical problems (see ref.[33] and references therein). More than 20 natural and synthetic zirconium silicates are known and for about one-third of them the crystal structures have been solved. Some of the first hydrothermal syntheses of zirconosilicates were carried out by Maurice in 1949.[63] Baussy et al. summarise the early work in this field and report the hydrothermal synthesis of (among others) analogues of the minerals catapleiite ($Na_2ZrSi_3O_9 \cdot 2\ H_2O$) and elpidite ($Na_2ZrSi_6O_{15} \cdot 3\ H_2O$) at 350–500 °C.[64] These materials have also been prepared by others.[65] Jale et al. reported the hydrothermal synthesis of a potassium analogue of elpidite at a relatively low temperature (200 °C).[32] The characteristic feature of the structure of elpidite is the presence of double chains of tetrahedra (epididymite type) connected by zirconium atoms in octahedral coordination (Figure 8a and 8b). The silicate chains form an anionic framework that is saturated by sodium ions. The double chains of tetrahedra are parallel to [100]. Two independent Na^+ cations are present. Na(2) has an octahedral coordination formed by four oxygens of the tetrahedra and two symmetrically equivalent water molecules. Na(1) occurs in a cavity formed by adjacent double chains of tetrahedra and it is bonded to seven oxygens and a water molecule.[66]

Recently, an excellent example of the interesting and promising chemistry of sodium zirconosilicates has been given by Clearfield et al.[33] These workers reported the synthesis, characterisation, and properties of three novel layered materials and five other zirconosilicates. In particular, a synthetic analogue of the mineral gaydonnayite (ideal formula $Na_2ZrSi_3O_9 \cdot 2\ H_2O$) has been prepared. This material has also been synthesised by Rocha and Anderson and co-workers (AV-4)[31] and by Jale et al.[32] The framework of gaydonnayite is composed of sinusoidal single chains of SiO_4 tetrahedra, repeating every six tetrahedra (Figure 8c and 8d).[67] The chains are extend alternately along [011] and [01–1] and are cross-linked by a ZrO_6 octahedron and two distorted NaO_6 octahedra.

Another interesting example of a microporous zirconosilicate is petarasite and its synthetic analogue AV-3.[31,68,69] This rare mineral $[Na_5Zr_2Si_6O_{18}(Cl,OH) \cdot 2\ H_2O]$ possesses a very unusual structure consisting of an open three-dimensional framework built of corner-sharing six-membered rings and ZrO_6 octahedra (Figure 8e and 8f).[68] Elliptical channels (3.5 × 5.5 Å) defined by mixed six-membered rings, consisting of pairs of SiO_4 tetrahedra linked by zirconium octahedra, run parallel to the *b* and *c* axes. Other channels limited by six-membered silicate rings run parallel to the *c* axis. The sodium, chloride and hydroxyl ions and the water molecules reside within the channels. The framework does not collapse until the release of Cl^- at ca. 800 °C.

The preparation of synthetic umbite materials has already been discussed in this microreview. The chemistry of other fascinating microporous framework solids is waiting to be explored. For instance, the mineral lemoynite, $(Na,K)_2CaZr_2Si_{10}O_{26} \cdot 5–6\ H_2O$, possesses a $ZrSi_5O_{13}$ framework with wide open channels where sodium, potassium and calcium cations and water molecules reside.[70] This framework comprises thick (7 Å) layers of hexagons of silicate groups. The sheets are bound together by six-coordinated zirconium atoms. The hexagons are tilted with respect to the layer (001) plane and the architecture of these layers is new.

Niobosilicates

Comparatively few studies are available on microporous framework niobosilicates. In this microreview we have already discussed the work carried out on nenadkevichite analogues containing titanium and niobium.[45,46] Recent work suggests that other niobosilicate materials that show potential as heterogeneous catalysts are yet to be discovered. For example, Rocha and Anderson and co-workers have reported the synthesis of AM-11, a novel microporous sodium niobosilicate.[71] Although its structure is still unknown, this material has a relatively large pore volume and seems to contain NbO_6 octahedra and local silicon environments Si(4Si, 0Nb), Si(3Si, 1Nb) and Si(2Si, 2Nb). A preliminary characterisation of the acid-base properties has shown that AM-11 dehydrates *tert*-butyl alcohol to isobutene with remarkably high activity and selectivity.

Stannosilicates

The hydrothermal synthesis of microporous framework stannosilicates has been pioneered by Corcoran et al. As pointed out by these workers, several minerals containing SnO_6 and SiO_4 polyhedra are known and a few (dense)

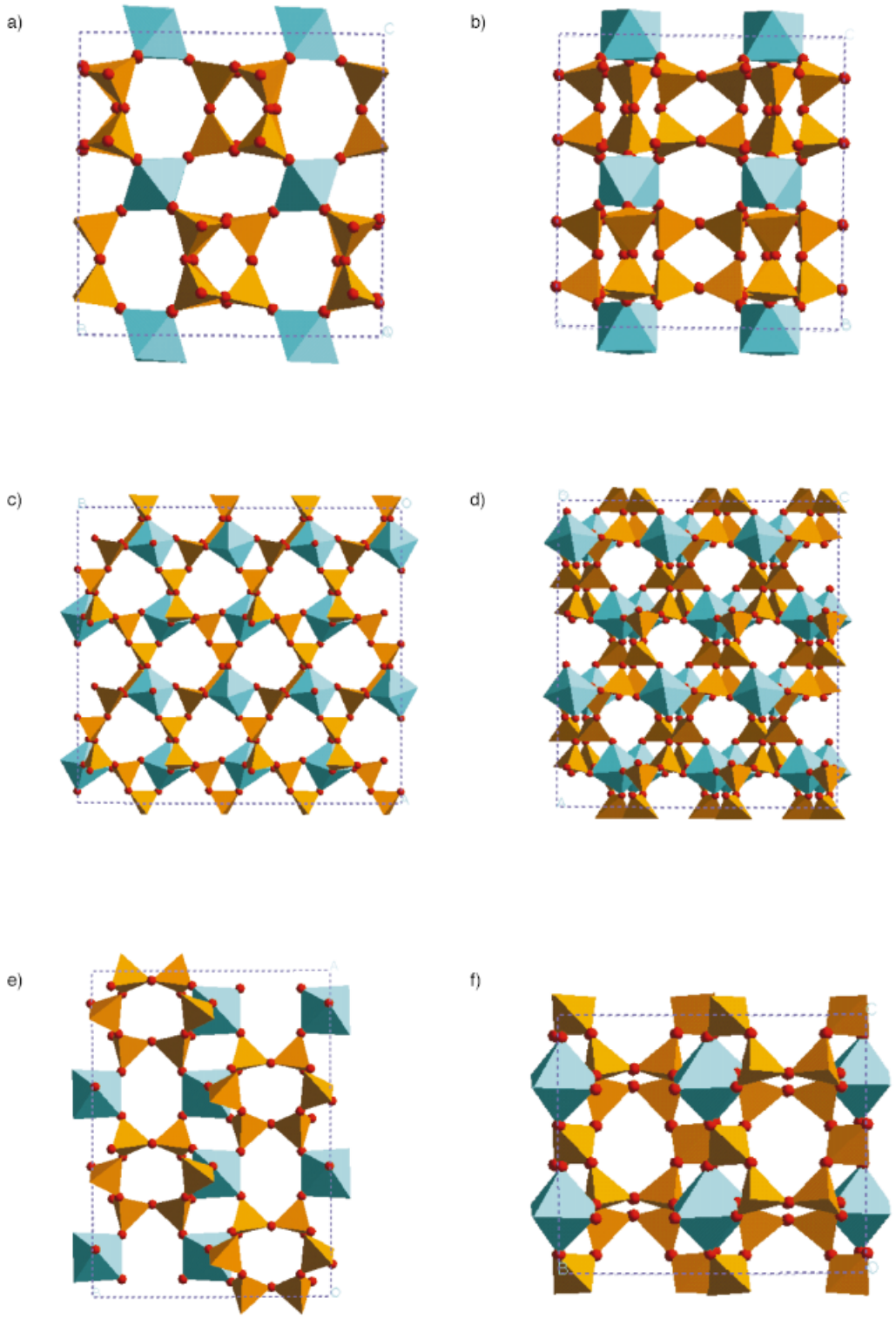

Figure 8. Projections of the structure of: (a) elpidite along the [100] and (b) [010] directions; (c) gaydonnayite and AV-4 along [001] and (d) [010]; (e) petarasite and AV-3 along [001] and (f) [100] directions; blue Zr octahedra, brown Si tetrahedra, red spheres oxygens

stannosilicate phases have been crystallised from high-temperature conditions.[72,73] Two microporous stannosilicates have been reported by Corcoran et al. The orthorhombic phase Sn-A has the composition $Na_8Sn_3Si_{12}O_{34} \cdot n\,H_2O$, while Sn–B has been formulated as $Na_4SnSi_4O_{12} \cdot n\,H_2O$. These materials show reversible water loss and have a significant ion-exchange capacity. A third, layered, stannosilicate ($Na_4SnSi_5O_{14} \cdot n\,H_2O$) has also been reported.[72] Subsequently, Dyer and Jafar reported the synthesis, characterisation and cation-exchange properties of a microporous stannosilicate with a very unusual habit and of composition $Na_{13.5}Sn_{10}Si_{15}O_{36}(OH)_5 \cdot 13.5\,H_2O$.[74] The ion-exchange

behaviour has been shown to be zeolitic in character. The crystal structures of all these solids are, as yet, unknown. Recently, Rocha et al. reported the synthesis and characterisation of two stannosilicates possessing the structures of titanosilicates umbite and UND-1 (Figure 7f).[75]

Vanadosilicates

Although vanadium has already been introduced into the framework of certain zeolites in small amounts, to the best of our knowledge only three microporous framework vanadosilicates are known to contain stoichiometric amounts of vanadium.[34,76,77] Canvasite and pentagonite, dimorphs of the mineral $Ca(VO)(Si_4O_{10}) \cdot 4\,H_2O$, have a framework formed by silicate layers of four- and eight-membered rings of tetrahedra connected vertically by V^{IV} cations that are in a square-pyramidal coordination (Figure 9).[76,77] Replacement of the VO_5 groups by two bridging oxygens would produce a tetrahedral framework topologically identical to that of the zeolite gismondine. The calcium cations and the water molecules reside in the channels formed by the eight-membered rings and between the SiO_2 layers. Canvasite has channels running parallel to the *c* direction with a free diameter of only 3.3 Å in the hydrated state. Hence, both canvasite and pentagonite are likely to behave (at best) as small-pore materials.

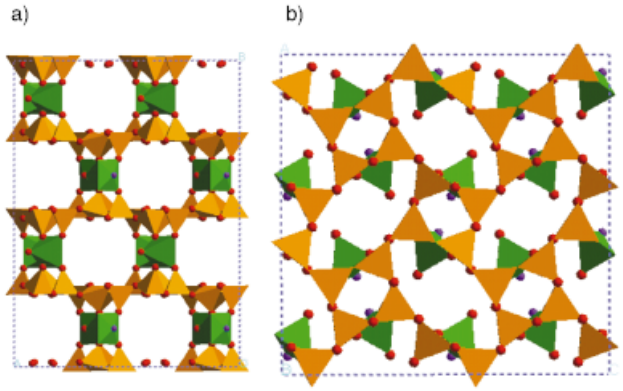

Figure 9. Projection of the structure of canvasite along the (a) [001] and (b) [010] directions; green V square pyramids, brown Si tetrahedra, red spheres oxygens

Recently, the synthesis and structural characterisation of the first large-pore vanadosilicate containing octahedral vanadium and possessing a structure similar to that of titanosilicate ETS-10 has been reported. The presence of stoichiometric amounts of vanadium in the framework of AM-6 gives this material great potential for applications as a catalyst, sorbate or functional material.[34]

Other Silicates

The synthesis of microporous framework silicates of a few other metals have been reported. One such case is AV-1, the synthetic analogue of the rare mineral montregianite (also known as UK-6).[78,79] This is an yttrium silicate, with the formula $Na_4K_2Y_2Si_{16}O_{38} \cdot 10\,H_2O$, that possesses a very unusual structure consisting of two different types of layers alternating along the [010] direction (Figure 10a and 10b):[80] (a) a double silicate sheet, where the single silicate sheet is of the apophyllite type with four- and eight-membered rings, and (b) an open octahedral sheet composed of $[YO_6]$ and three distinct $[NaO_4(H_2O)_2]$ octahedra. The layers are parallel to the (010) plane. The K^+ ions are ten-coordinate and the six water molecules are located within large channels formed by the planar eight-membered silicate rings.

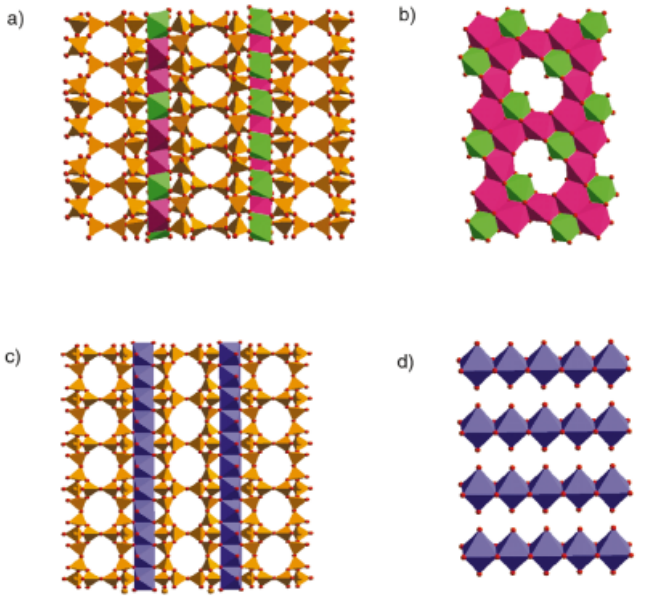

Figure 10. Projection of the structures of: (a) montregianite and AV-1 along the [001] direction; (b) one octahedral layer seen along the [010] direction; (c) rhodesite and AV-2 along [010]; (d) one octahedral layer seen along [100]; green Y octahedra, red Na octahedra, blue Ca octahedra, brown Si tetrahedra, red spheres oxygens

The structure of the alkali calcium silicate mineral rhodesite ($HKCa_2Si_8O_{19} \cdot 6\,H_2O$)[81] and its synthetic analogue AV-2[79] is closely related to that of montregianite. It consists of silicate double layers, chains of edge-sharing $[Ca(O,OH_2)_6]$ octahedra and potassium cations, and additional water molecules within the pores of the silicate double layers (Figure 10c and 10d). Rhodesite and montregianite have double silicate layers of the same topology. In fact, other minerals such as delhayelite, hydrodelhayelite and macdonaldite, all have similar double silicate sheets. In rhodesite these layers possess the maximum topological symmetry (*P*2*mm*) while in montregianite all symmetry has been lost. The structure of rhodesite contains two sets of octahedrally-coordinated calcium ions, which form single chains parallel to [001]. The octahedral chains connect adjacent silicate double layers. While Ca(2) is coordinated to six terminal oxygens that belong to six different SiO_4 tetrahedra, Ca(1) is coordinated to four terminal oxygens from four SiO_4 and two oxygens from water molecules. The extra-framework potassium ions are ten-coordinated to six bridging oxygens and four water molecules.

Characterisation

Disorder

The structures of many microporous materials are disordered and this is the case for the important microporous titanosilicates ETS-10 and ETS-4. It can be assumed that it is likely that a number of the new structures, which will undoubtedly be synthesised in the future, will also be disordered. Disorder should be distinguished from defects. Disorder usually results from the apparent intergrowth of different polymorphs of a structure. In the ideal case this will occur without a disruption in the connectivity of the framework, i.e. internal –OH groups will not be present. Sometimes disorder causes the apparent diffusion pathway through the channel system to be disrupted, as with ETS-4,[39] but sometimes the disorder causes no disruption, as with ETS-10.[13,14] Characterisation of such disordered structures can be complicated, especially if the materials can only be crystallised as microcrystalline powders. The following gives a short description of how a range of characterisation techniques can be powerfully focussed on the problem of characterising disordered materials.

Bulk characterisation techniques generally fall into two categories: those that concern short range effects and those that concern long range effects. This is an important distinction when characterising disordered materials as often, although by no means always, the disorder is manifested beyond the short-length scale. If the disorder occurs on a length scale of tens of Ångstroms, short-range techniques such as high-resolution electron microscopy (HREM), solid-state nuclear magnetic resonance with magic-angle spinning (MAS NMR), infrared spectroscopy (IR), Raman spectroscopy, electronic spectroscopy, and extended X-ray absorption fine structure (EXAFS) will give high quality data. These techniques will behave in the same manner as if there was no disorder. All diffraction techniques, which are inherently long-range techniques, will reflect both the structure and disorder in the material. Consequently, it is often sensible to begin with the short-range techniques and HREM in particular can give information about the possible pore structure and also about how disorder and defects may be incorporated within the material. This is often the cornerstone of any structural analysis. Local chemical environments may be probed in a quantitative fashion using MAS NMR and ^{29}Si is often a useful nucleus in this respect.[82] In favourable circumstances this technique will also yield crystallographic distinctions within a chemical grouping. All these new microporous phases will contain counterbalancing cations and these are often particularly difficult to locate in a disordered material. A common counterbalancing cation is sodium, which is a particularly good NMR nucleus. Because of the quadrupolar nature of ^{23}Na a number of sophisticated modern experiments have been developed known as multiple-quantum NMR spectroscopy. Infrared and Raman spectroscopies can often reveal structural units within a framework. Electronic spectroscopy will show the existence of band gaps, which can be characteristic of certain structures. EXAFS is a useful tool for homing in on a structure towards the end of an analysis. Because of the inability of this technique to distinguish different sites, the data obtained is a composite for the whole sample and is usually of little use in the early stages of structural characterisation. However, EXAFS will reveal very accurate bond lengths in a structure. EXAFS studies on ETS-10 have shown that within the titanate chain the Ti–O bonds are alternately long and short.[35] This will have marked consequences for optical properties.

In the case of ETS-10 this suite of short-range techniques was sufficient to ascertain a framework connectivity for the structure.[13,14] Atomic coordinates can then be refined using simple geometric constraints (bond angles and bond lengths). This is known as a distance-least-squares (or DLS) approach. With suitable interatomic potentials, which exist for titanosilicates[83] but not for some of the more exotic elements, energy minimisation can also be used to refine atomic coordinates. At this stage simulation of HREM images provides one of the best ways to confirm the trial structure.[84]

The diffraction data can be handled in two ways. Usually the diffraction data will consist of sharp and diffuse reflections that are characteristic of the underlying structure and the disorder. By concentrating solely on the sharp reflections it is sometimes possible to define a superposition cell. This is a unit cell that contains structural units in all possible configurations owing to the disorder. Consequently, the unit cell so defined will contain a superposition of framework units with some displacement characteristic of the disorder.

Alternatively the disorder can be incorporated into the calculation of the diffraction data, and a particularly powerful method in this regard is DIFFaX, a technique designed by Treacy, Newsam and Deem in 1991.[85] In this method the structure is built up from structurally perfect layers that are connected according to suitable rules to define the particular disorder observed for the material of interest. In this manner both sharp and diffuse reflections can be simulated. At present it is not possible to use this technique in an iterative fashion, such as Rietveld refinement, and consequently it is best used to confirm structure rather than refine structure.

Isomorphous Framework Substitution

The insertion of heteroatoms into the framework of microporous materials is an important process because it allows the fine-tuning of the their properties. Despite the fact that a considerable amount of work has been carried out on zeolites and other related systems, obtaining unequivocal evidence for framework substitution is not a trivial task and it usually requires the combined use of several techniques. Detailed studies on framework insertion of aluminium, gallium, boron, and niobium on ETS-10 have been reported and we will summarise in the following.

In an attempt to improve the acid characteristics of ETS-10 (and following up the early synthesis work by Kuznicki et al.[28,29]) Rocha and Anderson and co-workers have incorporated aluminium[86,87] and gallium[24,87] into tetrahed-

ral silicon sites, thus generating sites for zeolite-type acidity. These materials are known as ETAS-10 and ETGS-10, respectively. The main evidence for the substitution of silicon by aluminium and gallium in the framework of ETS-10 is provided by solid state NMR. The ^{29}Si MAS-NMR spectra of ETS-10, ETAS-10, and ETGS-10 are shown in Figure 11.

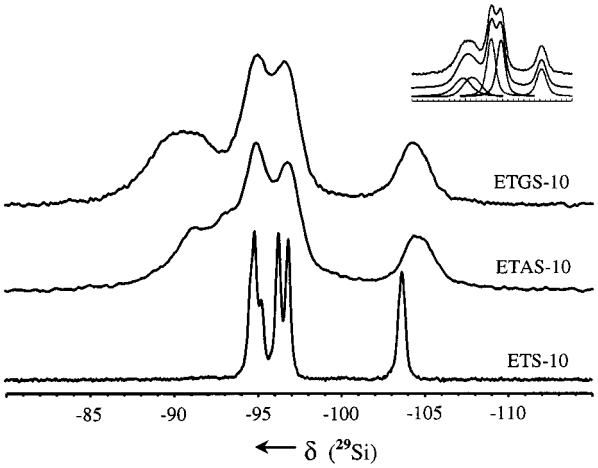

Figure 11. ^{29}Si MAS-NMR spectra of ETS-10, ETAS-10 and ETGS-10; the inset shows a deconvolution of the ETGS-10 spectrum

In ETS-10 there are two types of silicon chemical environments, Si(3Si, 1Ti) and Si(4Si, 0Ti), which give rise to the two groups of resonances at δ = –94 to –97 and ca. –103.7, respectively. The ratio of these environments is 4:1. The spectrum reveals a further crystallographic splitting of the Si(3Si, 1Ti) site. The spectrum of ETAS-10 contains all the ETS-10 resonances plus two other peaks ca. 4 ppm downfield from the Si(3Si, 1Ti) signals. These new peaks become stronger when the framework aluminium concentration increases (Figure 12).

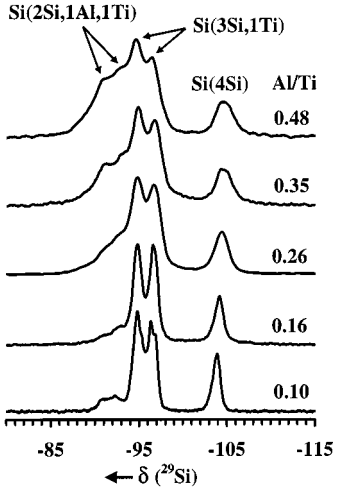

Figure 12. ^{29}Si MAS-NMR spectra of ETAS-10 with the Al/Ti ratios depicted

These signals are ascribed to the framework incorporation of aluminium to produce Si(2Si, 1Al, 1Ti) environments. It is important to note that there is no signal ca. 4 ppm downfield from the Si(4Si, 0Ti) resonance, showing no aluminium substitution neighbouring this silicon site and, hence, providing direct evidence for Al, Ti avoidance.[24,86]

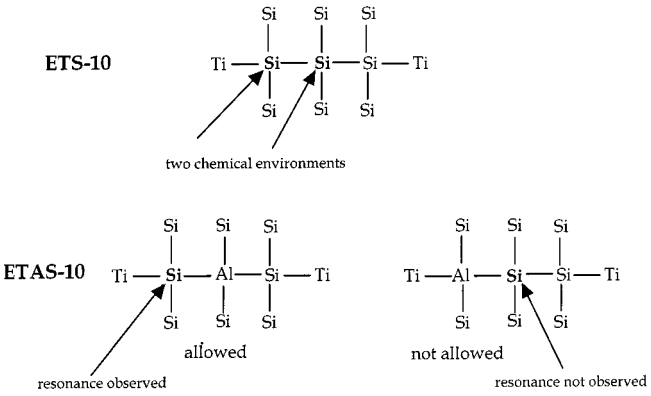

The ^{27}Al MAS-NMR spectrum (not shown) is also indicative of this effect since it contains a single resonance at δ ≈ 60, which is assigned to Al(4Si).

The ^{29}Si MAS-NMR spectrum of gallium-substituted ETS-10 resembles the spectrum of ETAS-10: a broad peak is seen downfield from the Si(3Si, 1Ti) signals. This peak can be deconvoluted into two component signals, each one ca. 1.5 ppm downfield from the Si(2Si, 1Al, 1Ti) resonances, which we assign to Si(2Si, 1Ga, 1Ti) as similar downfield shifts of the ^{29}Si NMR resonances have been reported for gallium-substituted zeolites. No signals are observed in the range δ = –99 to –103.[24,86] On the other hand, the ^{71}Ga MAS-NMR spectrum of fully-hydrated ETGS-10 (not shown) displays a broad peak at δ = 160, which is characteristic of four-coordinated gallium.

Detailed analysis of spectral intensities (I_{Si}) allows framework Si/Al (or Si/Ga) and Si/Ti ratios to be calculated from Equation 1 and Equation 2.

$$\mathrm{Si/Al} = \frac{\sum_{n=0}^{4-m}\sum_{m=0}^{4-n} \mathrm{I}_{\mathrm{Si(nAl,mTi)}}}{0.25\sum_{n=0}^{4-m}\sum_{m=0}^{4-n} \mathrm{nI}_{\mathrm{Si(nAl,mTi)}}} \quad (1)$$

$$\mathrm{Si/Ti} = \frac{\sum_{n=0}^{4-m}\sum_{m=0}^{4-n} \mathrm{I}_{\mathrm{Si(nAl,mTi)}}}{0.25\sum_{n=0}^{4-m}\sum_{m=0}^{4-n} \mathrm{mI}_{\mathrm{Si(nAl,mTi)}}} \quad (2)$$

Increasing the aluminium content in ETAS-10 broadens considerably the ^{29}Si-NMR resonances (Figure 12). In particular, the peak at δ = –104.5 becomes very broad, increasing its Full-Width-at-Half-Maximum (FWHM) from 40 Hz in ETS-10 to 200 Hz in ETAS-10 with Al/Ti = 0.48.[24] In fact, there is an almost perfectly linear correlation between the FWHM of this resonance and the Al/Ti ratio (equivalent to the aluminium content as aluminium replaces silicon and not titanium) of samples. In the case of zeolites the NMR lines are broadened for a number of reasons. Structural disorder, for example, gives rise to a dispersion of chemical shifts. Another important line broadening mech-

anism is the decrease of the spin-spin relaxation times brought about by $^{29}Si/^{27}Al$ dipolar interactions.[88] In order to assess this possibility the spin-spin relaxation times of an ETAS-10 sample with Si/Al = 0.24 has been measured. The two resonances at high frequency have short T_2 times (about 5 ms), confirming their assignment to silicons with aluminium neighbours and, thus, providing further evidence for framework substitution. The peaks attributed to Si(3Si, 1Ti) and Si(4Si) environments have similar, much longer relaxation times (35–49 ms). Therefore, the broadening of the Si(4Si) resonance cannot be explained by the dipolar mechanism discussed above. This effect is most likely caused by the distortion of the lattice upon aluminium incorporation.[86]

It is too early to say whether Al (Ga), Ti avoidance is a general phenomenon in titanoalumino(gallo)silicates. However, it seems logical that, wherever possible, Al (Ga) and Ti will not be neighbours. We have found that at relatively high Al and Ga framework concentrations slight deviations from the Al (Ga), Ti avoidance rule are observed.

The insertion of boron into ETS-10, yielding ETBS-10, has also been reported.[89] As the amount of boron in ETBS-10 increases, a new ^{29}Si MAS-NMR peak, attributed to Si–O–B environments, grows at $\delta \approx -99$ and (as in ETAS-10 and ETGS-10) all the resonances broaden considerably (not shown). On the other hand, the ^{11}B MAS-NMR spectra (not shown) of ETBS-10 samples with different boron contents are similar and contain two groups of very sharp peaks (FWHM ca. 78 Hz) at $\delta \approx -1.4$ and –2.9. This implies that any electric field gradients created by the electronic cloud at the ^{11}B nuclei are very small (quadrupole coupling constant estimated at 40–80 kHz) and shows that boron is in a tetrahedral, rather than a trigonal, coordination and replaces silicon in the framework of ETBS-10. Indeed, it has been reported that hydrated boron-substituted H-ZSM-5 zeolite gives a single sharp ^{11}B-NMR peak at $\delta = -3$.[90] On the other hand, the local environment of any extra-framework boron would, in principle, be more distorted or, at least, a dispersion of boron sites would occur leading to significantly broader ^{11}B MAS-NMR resonances.[89]

The insertion of niobium into the framework of ETS-10, replacing titanium, has been reported to pose particular problems because NMR does not provide strong evidence for it.[91] Indeed, only a relatively small broadening of the ^{29}Si MAS-NMR resonances is observed. In addition, the ^{93}Nb MAS-NMR spectrum recorded with a very fast (32 kHz) spinning rate displays a broad peak at $\delta = 100$ relative to solid Nb_2O_5, suggesting the presence of niobium in a distorted octahedral coordination. However, Raman and FTIR spectroscopies provide strong evidence for this framework substitution. ETS-10 gives a strong and sharp main Raman band at ca. 735 cm^{-1}, assigned to the TiO_6 octahedra (not shown).[91] As the niobium content of the samples increases, this peak shifts slightly and broadens and, simultaneously, a band grows at ca. 664 cm^{-1}. The latter band is typical of NbO_6 octahedra in microporous niobosilicates. The FTIR spectrum of ETS-10 (not shown) displays bands at 446, 550, and 746 cm^{-1}, associated with the TiO_6 octahedra. As the niobium content of the samples increases the intensity of these bands decreases, while a new band at 918 cm^{-1} is seen. This is a further indication that niobium replaces titanium in the ETS-10 framework.

The great (largely overlooked) potential presented by Raman spectroscopy for studying the isomorphous framework substitutions in zeolite-type materials is particularly well illustrated by the synthetic titano-niobosilicate nenadkevichite system.[44,45] The Raman spectra of a sample with Ti/Nb = 0.8 (Figure 13) displays two main bands at 668 and 226 cm^{-1} associated with the NbO_6 octahedra. With increasing titanium content the intensity of these bands decreases (particularly of the former) while simultaneously two other strong bands grow at 764 and 290 cm^{-1}. These bands are attributed to NbO_6 octahedra.

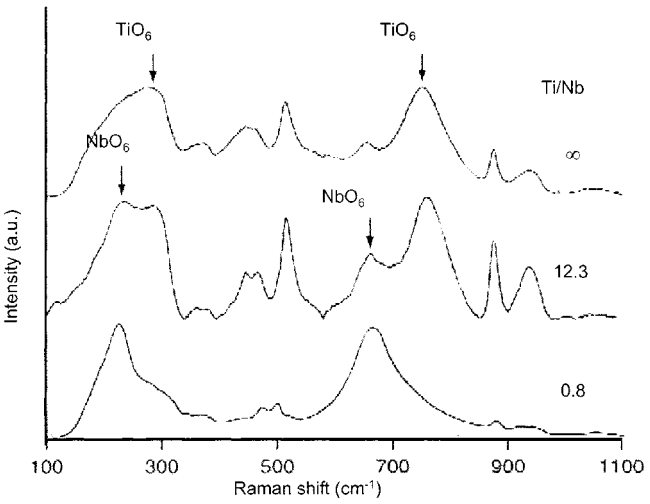

Figure 13. Raman spectra of synthetic nenadkevichite materials; the Ti/Nb ratios are indicated

The titanium for zirconium substitution in synthetic umbite has been studied in detail by powder X-ray diffraction.[31] It has been found that with increasing titanium content the unit cell shrinks in the three directions and its volume decreases systematically from ca. 985 (purely zirconeous sample) to 919 $Å^3$ (titaneous sample). This is not unexpected because Ti^{IV} is smaller than Zr^{IV}. ^{29}Si MAS-NMR spectroscopy provides further evidence for this framework substitution.[31] In the structure of umbite there are three types of Si(2Si, 2Zr) sites with populations 1:1:1.[50] The spectrum of purely zirconeous AM-2 displays a single broad peak at $\delta = -86.5$. In contrast, the spectrum of the purely titaneous sample contains a resonance at $\delta = -87.3$ and two overlapping peaks at about $\delta = -86.2$ and –85.9 in an approximate 1:1:1 intensity ratio, in accord with the crystal structure of umbite. Along the series, it is observed that as the zirconium content of the samples increases, the peak at about $\delta = -86.5$ broadens while the resonance at $\delta = -87.3$ broadens and eventually disappears from the spectrum.

Cation Location (Multiple-Quantum NMR and Computer Modelling)

The framework of these novel microporous materials is anionic and the charge density can be very high. Consider ETS-10, which has a basic formula unit of $Si_{40}Ti_8O_{104}^{16-}$. In other words there are 16 unit charges per 48 metal centres, which would be equivalent to a zeolite with a Si/Al ratio of 2 (which for zeolites is close to the Lowensteinian limit of Si/Al = 1). Moreover, the framework charge centres (at the octahedral Ti^{IV} site) carry an overall two-minus charge. Consequently, the charge distribution is quite different to the monovalent sites in the aluminosilicate zeolites. This will potentially make titanosilicates in this new class particularly attractive for exchanging divalent cations and are indeed particularly selective for some divalent heavy metals such as Pb^{2+} and Cd^{2+}.[9,92] Other materials reported above have an even higher charge density than the theoretical limit for zeolites, e.g. nenadkevichite with a composition $(Na,Ca)(Nb,Ti)Si_2O_7 \cdot H_2O$ is equivalent to a zeolite with Si/Al = 0.5.

It is desirable to characterise the cation site both in terms of crystallographic location and interaction with adsorbed molecules. For quadrupolar cations, such as sodium, the new technique of multiple-quantum MAS NMR is particularly powerful. Historically the NMR study of quadrupolar nuclei has been plagued by the inability to remove the quadrupole interaction, thereby gaining sufficient resolution to observe all possible sites. Two experimentally demanding techniques, dynamic angle spinning (DAS)[93] and double rotation (DOR),[94] were invented to overcome this problem but neither is easily implemented. Recently the technique of multiple-quantum (MQ) MAS NMR has provided a relatively straightforward solution to the problem.

The basic theory behind MQ MAS NMR is now well documented[95–98] and, thus, the following is a brief general overview. Consider the observation of a half-integer ($I > {}^1/_2$) spin nucleus. For a powdered sample, under fast spinning conditions, the frequency for symmetrical (m, $-m$) multiple-quantum transitions involves second- and fourth-rank angular dependent terms. The Legendre polynomials, P_2 and P_4, describing these angular dependencies are (Equation 3 and Equation 4)

$$P_2(\cos\theta) = \left(3\cos^2\theta - 1\right)/2 \quad (3)$$

$$P_4(\cos\theta) = \left(35\cos^4\theta - 30\cos^2\theta + 3\right)/8 \quad (4)$$

where θ is the angle between the spinning axis and the magnetic field B_0. As there is no common root to these polynomials, there is no single spinning axis that can completely remove the second-order quadrupolar broadening.

In the MQ MAS-NMR experiment the sample is spun at the magic angle and the magnetisation evolves sequentially under the triple (or quintuple) quantum Hamiltonian in the first part of time t_1 and under the single-quantum Hamiltonian during the second part. Judicious choice of the length of these evolution periods generates an isotropic echo. The simplest two-dimensional experiment is a two-pulse sequence whereby the pulse phases are cycled in an appropriate manner to select the desired quantum coherence. The projection of the (sheared) MQ MAS NMR spectrum onto axis F1 yields an isotropic, highly resolved spectrum, while the F2 projection is essentially the "conventional" MAS NMR spectrum. The position and profile of a peak in this two-dimensional spectrum immediately yields the isotropic chemical shift for the signal as well as the quadrupole coupling constant, C_Q, and the asymmetry parameter, η. These last two parameters define the quadrupole interaction, which is determined by the local environment of the nucleus. Conversely, if the environment is known then C_Q and η can be determined and compared with the NMR experiment.

Experimentally the technique is straightforward to implement. The hardware required is a conventional MAS NMR probe with smaller coil widths preferred in order to generate large radio-frequency fields. 4 mm rotors or even 2.5 mm rotors are preferable although there is a balance between sensitivity loss and gaining a high radio-frequency field. If the radio-frequency field is insufficient it will not be possible to excite nuclei experiencing a large quadrupolar interaction. These are generally highly coordinated nuclei in a very asymmetric environment.

A combination of MQ MAS NMR and computer modelling has been used to determine the sodium cation siting in ETS-10.[99–101] The ^{23}Na triple-quantum (3Q) MAS NMR spectrum of as-prepared ETS-10 is shown in Figure 14a and comprises two signals. Deconvolution of the isotropic sum projection onto F1 shows them to be in the ratio 2.6:1. The stronger signal comprises two sites, as evidenced by the shoulder in the isotropic F1 projection, with estimated δ_{iso}s and second-order quadrupole effects (SOQEs), $\sqrt{[C_Q^2(1 + (\eta^2/3)]}$ of –7.6 and 1.1 MHz and –7.5 and 1.3 MHz. The weaker signal is equally as broad in F1 and is also likely to comprise more than one site having δ_{iso}s of ca. –1.6 and a SOQEs of ca. 1.7 MHz.

Upon dehydration the weaker of the two signals in the spectrum of the hydrated material has now shifts to a lower F2 frequency (Figure 14b). This is due to an important change in δ_{iso} and SOQE from –1.6 and 1.7 MHz in hydrated ETS-10 to –3.7 and 2.4 MHz, in dehydrated ETS-10. Any sites responsible for this signal are thus strongly affected by dehydration. Although the shape of the stronger signal is slightly altered, it remains unshifted. The two sites largely unaffected by sample dehydration are assigned to sites I and II, which are tucked away on either side of the 12-ring pore (see Figure 5). The change in the position of the weaker signal upon dehydration suggests that any sites that give rise to this signal must be in the vicinity of water molecules and are thus likely to be situated in the pore void. This signal is therefore attributed to sites III and V, which are located at the top of the 12-ring pore near a titanate chain and loosely bound somewhere within the pore, respectively. A number of similar MQ MAS NMR studies have been carried out on a whole range of these novel microporous phases and the results will be published shortly.

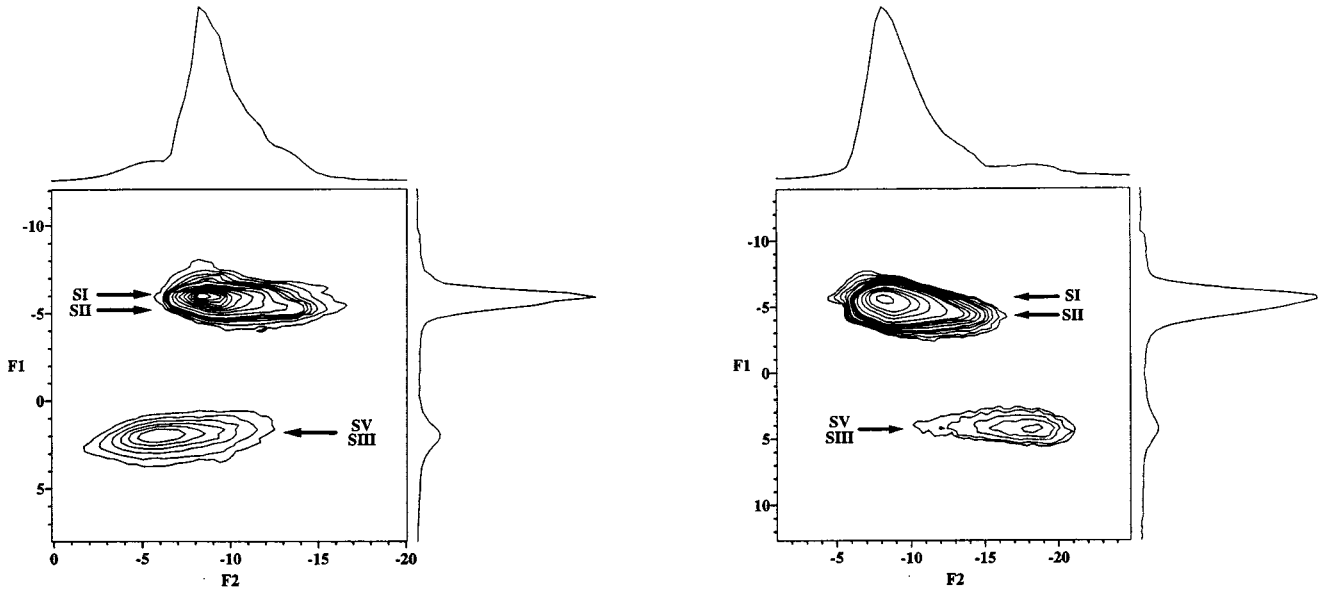

Figure 14. Triple-quantum ^{23}Na MAS-NMR spectra (9.4 T field) of ETS-10 (a) as-prepared and (b) dehydrated sample

Applications

Catalysis

For catalytic applications these novel framework materials present interesting new challenges. Apart from the possibilities for shape-selectivity and high activity through high surface area (similar to zeolites) these new materials possess a number of characteristics that make them particularly interesting as prospective heterogeneous catalysts. To date, only a moderate amount of work has been carried out on catalytic applications of the more stable wide-pore ETS-10 materials. However, this initial work is very encouraging and will no doubt be expanded greatly in the near future. For ETS-10 the catalytic applications have focused on the following attributes: high cation exchange capacity, which leads to many possibilities particularly in base catalysis; facile metal loading for bifuncionality; very low acidity; possible chiral activity; photocatalytic opportunities. It should be pointed out that the titanosilicates with octahedrally-coordinated titanium do not show good properties for oxidation catalysis in comparison to four-coordinate titanium. This is due to the ligand saturation, which prevents further attachment by oxidising agents such as hydrogen peroxide.

A number of papers by Bianchi, Ragaini, and co-workers detail Fischer–Tropsch chemistry over Co and Ru exchanged ETS-10.[102–105] The titanium silicate ETS-10 was found to be a suitable support for metal catalysts, due to its high surface area, high ion-exchange capability and the absence of an acidic function. The importance of alpha-olefin readsorption within the catalyst is discussed and the nature of this readsorption is tailored by effective control of the metal distribution inside the pores of ETS-10. The CO conversion and selectivity obtained also varies depending upon whether the active metal is introduced in the ETS-10 cages by ion-exchange or simply by impregnation.

Two groups, those of Anderson, Rocha, and co-workers[106] and Sivasanker and co-workers,[107–109] have studied the bifunctional reforming reaction of hexane to benzene over Pt-supported basic ETS-10. The basicity of the titanosilicate can be controlled by using samples exchanged with different alkali metals (M = Li, Na, K, Rb, or Cs). A distinct relationship between the intermediate electronegativity (S-int) of the different metal-exchanged ETS-10 samples and the yield of benzene is reported, suggesting the activation of Pt by the basicity of the exchanged metal. Typically ETS-10 samples exhibit greater aromatization activities than related Pt/Al_2O_3 catalysts. The very high basicity of ETS-10 in comparison with, for example zeolite X, is illustrated by Anderson and co-workers in a paper that discusses the relative conversion of 2-propanol to acetone.[110] The same group has also demonstrated how these same properties are effective in aldol chemistry[111] and dehydration of *tert*-butyl alcohol.[112,113] In this latter reaction conversions and selectivities close to 100% are observed at relatively modest temperatures.

One area of possible catalytic activity that has not yet been properly explored is the potential for photo-catalysis. In this respect, the activity of ETS-10 for the photocatalytic degradation of cyclohexanol, cyclododecanol, 2-hexanol, and benzyl alcohol is compared, by Fox and co-workers, with TiO_2 particles included within small and large pore zeolitic supports suspended in acetonitrile.[114] Although the activity was less than that displayed by the titanium-doped silicate TS-1 this work was reported before very much was known about the structure of ETS-10 and how it can be modified. Consequently, this field of research is ripe for exploration, particularly in terms of the optical properties of these novel materials.

Finally, ETS-10 offers the potential for chiral catalysis or asymmetric synthesis if the pure chiral polymorph of ETS-

10 can be synthesised. Along with zeolite β, ETS-10 is currently the only known wide-pore microporous material that possesses a chiral polymorph with a spiral channel. The structures of these as-prepared materials contain an equal proportion of intimately intergrown enantiomorphs and are consequently achiral. The task of synthesising a pure chiral polymorph is, of course, immense. However, with some of the recently developed molecular modelling techniques for designing suitable organic templates to direct the structure, it may well be possible to solve this problem in the next decade.[115]

Optical Properties

Owing to the presence of stoichiometric quantities of transition metals in the framework of these novel microporous materials, they have potential for interesting optical properties.[83,116–119] Most attention to date has again focussed on the microporous material ETS-10. The structure of ETS-10 contains –O–Ti–O–Ti–O– chains, with alternating long and short bonds, which are effectively isolated from each other by a silicate sheath. In effect, therefore, ETS-10 contains monoatomic –O–Ti–O–Ti–O– wires embedded in an insulating SiO_2 environment, a situation that leads to a one-dimensional quantum confinement of electrons or holes within this wire. A blue bandgap shift is associated with this charge carrier confinement within this unprecedented geometrical structure. The effective reduced mass, μ, of electrons and holes within this wire is calculated to be $1.66\ M(e) < \mu < 1.97\ M(e)$, which is consistent with a band gap of 4.03 eV and is quite different to that of bulk TiO_2. This work underlines the possible future role that these microporous materials may play in optoelectronic and nonlinear optical applications. The titanium within the chains can be readily reduced using Na vapour, which effects the following redox couple,[120]

$$Ti^{IV} + Na \rightarrow Ti^{III} + Na^+$$

thereby generating unpaired electrons within the titanate chain and also generating extra cation sites. After such reduction the material is not air stable and is easily reoxidised, generating additional Na_2O within the channels. Such redox couples also give strong indications of possible applications in battery technology.

Recently, Rocha et al. doped ETS-10 with Eu^{3+} and Er^{3+} by ion-exchange techniques and studied the luminescence properties of the resultant materials.[121–122] It has been found that only Eu^{3+}-doped ETS-10 is optically active. Upon calcination at temperatures in excess of 700 °C both materials transform into dense titanosilicate analogues of the mineral narsarsukite [$(Na, K)_2TiSi_4O_{11}$], which is made up of Si_4O_{10} chains that form tubes of rings consisting of four SiO_4 tetrahedra.[123] These tubes are linked by chains of corner-sharing TiO_6 octahedra. The cavities between the Si_4O_{10} tubes and octahedral chains contain Na^+, Eu^{3+} and Er^{3+} cations. Eu^{3+} and Er^{3+}-doped narsarsukite display very interesting luminescence properties. The latter, in particular, exhibits a high and stable room-temperature emission in the visible and in the infrared spectral regions. An efficient energy transfer between the narsarsukite skeleton and the optically active Er^{3+} centres seems to occur.[122]

Adsorption Properties

Dihydrogen, dinitrogen, carbon monoxide, and nitric oxide have all been adsorbed, at nominally liquid nitrogen temperature, on Na^+- and K^+- exchanged ETS-10.[124] IR spectroscopy indicates the formation of $M^+(H_2)$, $M^+(N_2)(n)$, $M^+(CO)(n)$ and $M^+(NO)$ (n = 1, 2, ...; M^+ = Na, K) adducts that prevalently involve alkali-metal cations located in the 12- membered channels. These adducts give main IR absorption bands in the range 4050–4150 cm^{-1} for H_2, 2331–2333 cm^{-1} for N_2, 2148–2176 cm^{-1} for CO, and 1820–1900 cm^{-1} for NO, which are assigned to the fundamental stretching mode of the diatomic molecules polarized by the electric field created by the metal ions. On Na-exchanged samples, the $Na^+(N_2)$ and $Na^+(CO)$ species, formed at the lowest dosage, evolve into $Na^+(N_2)(n)$ and $Na^+(CO)(n)$ (n = 2, 3) species upon increasing the gas phase pressure. This reversible "solvation" process is not observed for K-exchanged samples. There is no comparable precedent for this result for CO adsorbed on zeolites and it is indicative of the unique adsorption characteristics that can be expected with these highly charged, high cation capacity microporous materials.

Cation Exchange

To date there has been very little work on the cation exchange properties of this novel class of material. However, the cation exchange capacity is very high and, in addition, the framework anionic sites are typically divalent, which should be particularly useful for the exchange of divalent cations. Indeed ETS-10 has been shown to be particularly selective for Pb^{2+} [125] and Cd^{2+} [126] ions. Furthermore the penkvilksite structure has been shown to be particularly selective for Li^+ cations,[127] which again may indicate possible applications in battery technology.

Conclusions

In this review it has been shown that a new and exciting field of research into microporous zeotype solids is emerging. These stable silicate materials possess mixed octahedral-tetrahedral frameworks and display entirely new molecular architectures. Although much of the work performed to date has concentrated on titanosilicates, it is clear that the novel porous frameworks may contain many other elements, particularly transition metals such as Zr, Nb, Sn, V, and Y. We anticipate that some of the new materials will find applications in areas usually associated with zeolites. Others, however, may have potential applications in fields such as optoelectronics and nonlinear optics, batteries, magnetic materials and sensors.

Acknowledgments

We thank EC JOULE II (J. R. and M. W. A.), EPSRC (M. W. A.), FCT, PRAXIS XXI, and FEDER (J. R.) for financial support.

We are very grateful to Dr. O. Terasaki for helping to solve the structure of ETS-10 and for the fruitful collaboration between both our groups.

[1] D. W. Breck, *Zeolite Molecular Sieves*, John Wiley & Sons, New York, **1974**.
[2] R. M. Barrer, *Hydrothermal Chemistry of Zeolites*, Academic Press, New York, **1982**.
[3] R. Szostak, *Molecular Sieves*, Van Nostrand Reinhold, New York, **1989**.
[4] S. T. Wilson, S. Oak, B. M. Lok, E. M. Flanigen, W. Plains, US 4 310 440, **1982**.
[5] B. M. Lok, C. A. Messina, R. T. Gajek, T. R. Cannan, E. M. Flanigen, US 4 440 871, **1984**.
[6] S. T. Wilson, S. Oak, E. M. Flanigen, US 4 567 029, **1986**.
[7] [7a] S. L. Suib, *Curr. Opinion Solid State Mater. Sci.* **1998**, *3*, 63. – [7b] R. C. Haushalter, L. A. Mundi, *Chem. Mater.* **1992**, *4*, 31.
[8] D. M. Chapman, A. L. Roe, *Zeolites* **1990**, *10*, 730.
[9] S. M. Kuznicki, US Patent 4 853 202, **1989**.
[10] S. M. Kuznicki, US Patent 4 938 989, **1990**.
[11] D. M. Chapman, US Patent 5 015 453, **1990**.
[12] W. T. A. Harrison, T. E. Gier, G. D. Stucky, *Zeolites* **1995**, *15*, 408.
[13] M. W. Anderson, O. Terasaki, T. Oshuna, A. Philippou, S. P. Mackay, A. Ferreira, J. Rocha, S. Lidin, *Nature* **1994**, *367*, 347.
[14] M. W. Anderson, O. Terasaki, T. Oshuna, P. J. O'Malley, A. Philippou, S. P. Mackay, A. Ferreira, J. Rocha, S. Lidin, *Philos. Mag. B* **1995**, *71*, 813.
[15] T. K. Das, A. J. Chandwadkar, S. Sivasanker, *Chem. Commun.* **1996**, 1105.
[16] X. Liu, J. K. Thomas, *Chem. Commun.* **1996**, 1435.
[17] D. M. Poojary, R. A. Cahill, A. Clearfield, *Chem. Mater.* **1994**, *6*, 2364.
[18] J. Rocha, P. Brandão, Z. Lin, A. P. Esculcas, A. Ferreira, M. W. Anderson, *J. Phys. Chem.* **1996**, *100*, 14978.
[19] J. Rocha, A. Ferreira, Z. Lin, M. W. Anderson, *Microporous Mesoporous Mater.* **1998**, *23*, 1253.
[20] T. K. Das, A. J. Chandwadkar, A. P. Budhkar, A. A. Belhekar, S. Sivasanker, *Microporous Mater.* **1995**, *4*, 195.
[21] V. Valtchev, S. Mintova, *Zeolites* **1994**, *14*, 697.
[22] V. P. Valtchev, *J. Chem. Soc., Chem. Commun.* **1994**, 730.
[23] T. P. Das, A. J. Chandwadkar, A. P. Budhkar, S. Sivasanker, *Microporous Mater.* **1996**, *5*, 401.
[24] M. W. Anderson, A. Philippou, Z. Lin, A. Ferreira, J. Rocha, *Angew. Chem. Int. Ed. Engl.* **1995**, *34*, 1003.
[25] J. Rocha, Z. Lin, A. Ferreira, M. W. Anderson, *J. Chem. Soc., Chem. Commun.* **1995**, 867.
[26] J. Rocha, P. Brandão, J.D. Pedrosa de Jesus, A. Philippou, M. W. Anderson, *Chem. Commun.* **1999**, 471.
[27] J. Rocha, P. Brandão, M. W. Anderson, T. Ohsuna, O. Terasaki, *Chem. Commun.* **1998**, 667.
[28] [28a] S. M. Kuznicki, K. A. Thrush, US 5 244 650, **1993**. – [28b] S. M. Kuznicki, R. J. Madon, G. S. Koermer, K. A. Thrush, EPA 0405978A1, **1991**.
[29] S. M. Kuznicki, A. K. Thrush, WO91/18833, **1991**.
[30] J. Rocha, P. Ferreira, Z. Lin, J. R. Agger, M. W. Anderson, *Chem. Commun.* **1998**, 1268.
[31] Z. Lin, J. Rocha, P. Ferreira, A. Thursfield, J. R. Agger, M. W. Anderson, *J. Phys. Chem. B.* **1999**, *103*, 957.
[32] S. R. Jale, A. Ojo, F. R. Fitch, *Chem. Commun.* **1999**, 411.
[33] A. I. Bortun, L. N. Bortun, A. Clearfield, *Chem. Mater.* **1997**, *9*, 1854.
[34] J. Rocha, P. Brandão, Z. Lin, M. W. Anderson, V. Alfredsson, O. Terasaki, *Angew. Chem. Int. Ed. Engl.* **1997**, *36*, 100.
[35] G. Sankar, R. G. Bell, J. M. Thomas, M. W. Anderson, P. A. Wright, J. Rocha, A. Ferreira, *J. Phys. Chem.* **1996**, *100*, 449.
[36] X. Q. Wang, A. J. Jacobson, *Chem. Commun.* **1999**, 973.
[37] A. N. Mer′kov, I. V. Bussen, E. A. Goiko, E. A. Kul'chitskaya, Y. P. Men′shikov, A. P. Nedorezova, *Zap. Vses. Mineralog. O-va* **1973**, *102*, 54.
[38] P. A. Sandomirskii, N. V. Belov, *Sov. Phys. Crystallogr.* **1979**, *24*, 686.
[39] A. Philippou, M. W. Anderson, *Zeolites* **1996**, *16*, 98.
[40] G. Cruciani, P. DeLuca, A. Nastro, P. Pattison, *Microporous Mesoporous Mater.* **1998**, *21*, 143.
[41] M. Naderi, M. W. Anderson, *Zeolites* **1996**, *17*, 437.
[42] E. A. Behrens, D. M. Poojari, A. Clearfield, *Chem. Mater.* **1996**, *8*, 1236.
[43] P. G. Perrault, C. Boucher, J. Vicat, E. Cannillo, G. Rossi, *Acta Crystallogr., Sect. B* **1973**, *29*, 1432.
[44] J. Rocha, P. Brandão, Z. Lin, A. Kharlamov, M. W. Anderson, *Chem. Commun.* **1996**, 669.
[45] J. Rocha, P. Brandão, Z. Lin, A. P. Esculcas, A. Ferreira, M. W. Anderson, *J. Phys. Chem.* **1996**, *100*, 14978.
[46] Z. Lin, J. Rocha, P. Brandão, A. Ferreira, A. P. Esculcas, J. D. Pedrosa de Jesus, A. Philippou, M. W. Anderson, *J. Phys. Chem.* **1997**, *101*, 7114.
[47] D. M. Poojari, A. I. Bortun, L. N. Bortun, A. Clearfield, *Inorg. Chem.* **1997**, *36*, 3072.
[48] M. S. Dadachov, A. Le Bail, *Eur. J. Solid State Inorg. Chem.* **1997**, *34*, 381.
[49] X. Liu, M. Shang, J. K. Thomas, *Microporous Mater.* **1997**, *10*, 273.
[50] G. D. Ilyushin, *Inorg. Mater.* **1993**, *29*, 853.
[51] S. Merlino, M. Pasero, G. Artioli, A. P. Khomyakov, *Am. Mineral.* **1994**, *79*, 1185.
[52] Y. Liu, H. Du, F. Zhou, W. Pang, *Chem. Commun.* **1997**, 1467.
[53] Y. Liu, H. Du, Y. Xu, H. Ding, W. Pang, Y. Yue, *Microporous Mesoporous Mater.* **1999**, *28*, 511.
[54] R. K. Rastsvetaeve, V. I. Andrianov, *Kristallografiya* **1984**, *29*, 681.
[55] J. V. Smith, *Chem. Rev.* **1988**, *88*, 149.
[56] A. R. Kampf, A. A. Khan, W. H. Baur, *Acta Crystallogr., Sect. B* **1973**, *B29*, 2019.
[57] L. P. Solov'eva, S. V. Borisov, V. V. Bakakin, *Sov. Phys. Crystallogr. (Engl. Transl.)* **1972**, *16*, 1035.
[58] . Du, M. Fang, J. Chen, W. Pang, *J. Mater. Chem.* **1996**, *6*, 1827.
[59] M. A. Roberts, G. Sankar, J. M. Thomas, R. H. Jones, H. Du, M. Fang, J. Chen, W. Pang, R. Xu, *Nature* **1996**, *381*, 401.
[60] M. S. Dadachov, J. Rocha, A. Ferreira, M. W. Anderson, *Chem. Commun.* **1997**, 2371.
[61] A. Clearfield, A. I. Bortun, L. N. Bortun, R. A. Cahill, *Solvent Extr. Ion Exch.* **1997**, *15*, 285.
[62] A. I. Bortun, L. N. Bortun, A. Clearfield, *Solvent Extr. Ion Exch.* **1997**, *15*, 909.
[63] O. D. Maurice, *Econ. Geol.* **1949**, *44*, 721.
[64] G. Baussy, R. Caruba, A. Baumer, G. Turco, *Bull.Soc. fr. Minéral. Crystallogr.* **1974**, *97*, 433.
[65] G. Y. Chao, D. H. Watkinson, *Can. Mineral.* **1974**, *12*, 316.
[66] E. Cannillo, G. Rossi, L. Ungaretti, *Amer. Mineral.* **1973**, *58*, 106.
[67] G. Y. Chao, *Can. Mineral.* **1985**, *23*, 11.
[68] S. Ghose, C. Wan, G. Y. Chao, *Can. Mineral.* **1980**, *18*, 503.
[69] J. Rocha, P. Ferreira, Z. Lin, J. R. Agger, M. W. Anderson, *Chem. Commun.* **1998**, 1269.
[70] Y. Le Page, G. Perrault, *Can. Mineral.* **1976**, *14*, 132.
[71] J. Rocha, P. Brandão, A. Philippou, M. W. Anderson, *Chem. Commun.* **1998**, 2687.
[72] E. W. Corcoran Jr., D. E. W. Vaughan, *Solid State Ionics* **1989**, *32/33*, 423.
[73] E. W. Corcoran Jr., J. M. Newsam, H. E. King Jr., D. E. Waughan, *ACS Symp. Ser.* **1989**, *398*, 603.
[74] [74a] A. Dyer, J. J. Jafar, *J. Chem. Soc., Dalton Trans.* **1990**, 3239. – [74b] A. Dyer, J. J. Jafar, *J. Chem. Soc., Dalton Trans.* **1991**, 2639.
[75] [75a] Z. Lin, J. Rocha, A. Valente, *Chem. Commun.* in press. – [75b] Z. Lin, J. Rocha, A. Ferreira, *J. Mater. Chem.*, submitted.
[76] H. T. Evans Jr., *Amer. Mineral., Sect. B* **1973**, *58*, 412.
[77] R. Rinaldi, J. J. Pluth, J. V. Smith, *Acta Crystallogr., Sect. B* **1975**, *31*, 1598.
[78] J. Rocha, P. Ferreira, Z. Lin, P. Brandão, A. Ferreira, J. D. Pedrosa de Jesus, *Chem. Commun.* **1997**, 2103.
[79] J. Rocha, P. Ferreira, Z. Lin, P. Brandão, A. Ferreira, J. D. Pedrosa de Jesus, *J. Phys. Chem.* **1998**, *102*, 4739.
[80] S. Ghose, P. K. S. Gupta, C. F. Campana, *Am. Mineral.* **1987**, *72*, 365.

[81] K.-F. Hesse, F. Z. Liebau, *Kristallogr.* **1992**, *199*, 25.
[82] A. Labouriau, T. J. Higley, W. L. Earl, *J. Phys. Chem. B* **1998**, *102*, 2897.
[83] A. J. M. deMan, J. Sauer, *J. Phys. Chem.* **1996**, *100*, 5025.
[84] T. Ohsuna, O. Terasaki, D. Watanabe, M. W. Anderson, S. Lidin, *"Zeolites and Related Microporous Materials: State of the Art 1994" Stud. Surf. Sci. Catal.* (Eds.: Weitkamp et al.), **1994**, vol. *84*, p. 413.
[85] M. M. J. Treacy, J. M. Newsam, M. W. Deem, *Proc. Roy. Soc. London A* **1991**, *433*, 499.
[86] M. W. Anderson, J. Rocha, Z. Lin, A. Philippou, I. Orion, A. Ferreira, *Microporous Mater.* **1996**, *6*, 195.
[87] J. Rocha, Z. Lin, A. Ferreira, M. W. Anderson, *J. Chem. Soc., Chem. Commun.* **1995**, 867.
[88] M. W. Anderson, *Magn. Reson. Chem.* **1992**, *30*, 898.
[89] J. Rocha, P. Brandão, M. W. Anderson, T. Ohsuna, O. Terasaki, *Chem. Commun.* **1998**, 667.
[90] K. F. M. G. J. Scholle, W. S. Veeman, *Zeolites* **1985**, *5*, 118.
[91] J. Rocha, P. Brandão, J. D. Pedrosa de Jesus, A. Philippou, M. W. Anderson, *Chem. Commun.* **1999**, 471.
[92] M. W. Anderson, unpublished results.
[93] B. F. Chmelka, K. T. Mueller, A. Pines, J. Stebbins, Y. Wu, J. W. Zwanziger, *Nature* **1989**, *339*, 42.
[94] [94a] A. Samoson, E. Lippmaa, A. Pines, *Mol. Phys.* **1988**, *65*, 1013. – [94b] A. Llor, J. Virlet, *Chem. Phys. Lett.* **1988**, *152*, 248.
[95] L. Frydman, J. S. Harwood, *J. Am. Chem. Soc.* **1995**, *117*, 5367.
[96] J.-P. Amoureux, C. Fernandez, L. Frydman, *Chem. Phys. Lett.* **1996**, *259*, 347.
[97] C. Fernandez, J.-P. Amoureux, *Chem. Phys. Lett.* **1995**, *242*, 449.
[98] A. Medek, J. S. Harwood, L. Frydman, *J. Am. Chem. Soc.* **1995**, *117*, 12779.
[99] M. W. Anderson, J. R. Agger, D. P. Luigi, A. K. Baggaley, J. Rocha, *PCCP* **1999**, *1*, 2287.
[100] J. R. Agger, M. W. Anderson, J. Rocha, D. P. Luigi, M. Naderi, A. K. Baggaley, *Proc. 12th International Zeolite Conf., Baltimore* (Eds.: M. R. S. Treacey et al.), July **1998**, p. 2457.
[101] S. Ganapathy, T. K. Das, R. Vetrivel, S. S. Ray, T. Sen, S. Sivasanker, L. Delevoye, C. Fernandez, J. P. Amoureux, *J. Am. Chem. Soc.* **1998**, *120*, 4752.
[102] C. L. Bianchi, S. Vitali, V. Ragaini, *Stud. Surf. Sci. Catal.* **1998**, *119*, 167.
[103] C. L. Bianchi, S. Ardizzone, V. Ragaini, *Stud. Surf. Sci. Catal.* **1998**, *119*, 173.
[104] C. L. Bianchi, V. Ragaini, *J. Catal.* **1997**, *168*, 70.
[105] C. L. Bianchi, R. Carli, S. Merlotti, V. Ragaini, *Catal. Lett.* **1996**, *41*, 79.
[106] A. Philippou, M. Naderi, N. Pervaiz, J. Rocha, M. W. Anderson, *J. Catal.* **1998**, *178*, 174.
[107] S. B. Waughmode, T. K. Das, R. Vetrivel, S. Sivasanker, *J. Catal.* **1999**, *185*, 265.
[108] T. K. Das, A. J. Chandwadkar, S. Sivasanker, *Stud. Surf. Sci. Catal.* **1998**, *113*, 455.
[109] T. K. Das, A. J. Chandwadkar, H. S. Soni, S. Sivasanker, *Catal. Lett.* **1997**, *44*, 113.
[110] A. Philippou, J. Rocha, M. W. Anderson, *Catal. Lett.* **1999**, *57*, 151.
[111] A. Philippou, M. W. Anderson, *J. Catal.*, in press.
[112] A. Philippou, M. Naderi, J. Rocha, M. W. Anderson, *Catal. Lett.* **1998**, *53*, 221.
[113] T. K. Das, A. J. Chandwadkar, H. S. Soni, S. Sivasanker, *J. Mol. Catal. A – Chemical* **1996**, *107*, 199.
[114] M. A. Fox, K. E. Doan, M. T. Dulay, *Res. Chem. Intermed.* **1994**, *20*, 711.
[115] D. W. Lewis, D. J. Willock, C. R. A. Catlow, J. M. Thomas, G. J. Hutchings, *Nature* **1996**, *382*, 604.
[116] B. Mihailova, V. Valtchev, S. Minatova, L. Konstantinov, *Zeolites* **1996**, *16*, 22.
[117] Y. N. Xu, W. Y. Ching, Z. Q. Gu, *Ferroelectrics* **1997**, *194*, 219.
[118] E. Borello, C. Lamberti, S. Bordiga, A. Zecchina, C.O. Arean, *Appl. Phys. Lett.* **1997**, *71*, 2319.
[119] C. Lamberti, *Microporous Mesoporous Mater.* **1999**, *30*, 155.
[120] A. Zecchina, personal communication.
[121] J. P. Rainho, L. D. Carlos, J. Rocha, *J. Lumin.*, in press.
[122] J. Rocha, L. D. Carlos, J. P. Rainho, Z, Lin, R. M. Almeida, *J. Mater. Chem.*, submitted.
[123] Y. A. Pyatenko, Z. V. Pudvkina, *Kristallografiya* **1960**, *5*, 563.
[124] A. Zecchina, C. O. Arean, G. T. Palomino, F. Geobaldo, C. Lamberti, G. Spoto, S. Bordiga, *PCCP* **1999**, *1*, 1649.
[125] S. M. Kuznicki, K. A. Thrush, US Patent 4 994 191, **1991**.
[126] M. W. Anderson, M. Mohsen, unpublished results.
[127] S. M. Kuznicki, J. S. Curran, X. Yang, US Patent 5 882 624, **1999**.

Received October 12, 1999
[I99360]